Contract No:

This document was prepared in conjunction with work accomplished under Contract No. DE-AC09-08SR22470 with the U.S. Department of Energy (DOE) Office of Environmental Management (EM).

Disclaimer:

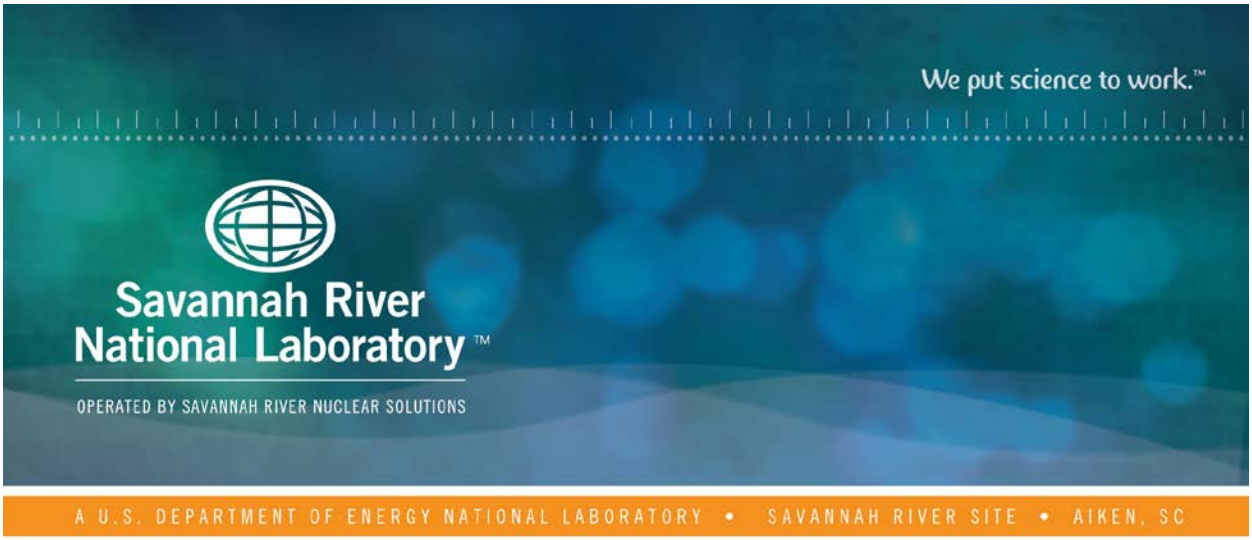

Annual Report, Spring 2015: Alternative Chemical Cleaning Methods for High Level Waste Tanks – Corrosion Test Results

R. B. Wyrwas

May 2015

SRNL-STI-2015-00302

DISCLAIMER

Printed in the United States of America

Prepared for
U.S. Department of Energy

SRNL-STI-2015-00302
Revision 0

Keywords: *enhanced chemical cleaning, corrosion, permanganate, oxalic acid, nitric acid, tank waste heel*

Retention:

ANNNUAL REPORT, SPRING 2015: ALTERNATIVE CHEMICAL CLEANING METHODS FOR HIGH LEVEL WASTE TANKS – CORROSION TEST RESULTS

R. B. Wyrwas

May 2015

Savannah River National Laboratory™
OPERATED BY SAVANNAH RIVER NUCLEAR SOLUTIONS

Prepared for the U.S. Department of Energy under contract number DE-AC09-08SR22470.

REVIEWS AND APPROVALS

AUTHOR:

_____

R. B.Wyrwas, Materials Performance and Corrosion Technology Date

TECHNICAL REVIEW:

_____

R.E. Fuentes, Materials Performance and Corrosion Technology Date

APPROVALS:

_____

B. J. Wiersma, Manager Date
Materials Performance and Corrosion Technology

_____

W. D. King, Program Lead Date
Advanced Characterization and Process

_____

E. N. Hoffman, Manager Date
Engineering Process Development

_____

A.P. Fellinger, Manager Date
Environmental & Chemical Process Technology Research Programs

_____

Gary R. Peterson, Manager Date
DOE Headquarters Program Manager

Table of Contents

1 Executive Summary 1
2 Background 2
3 Experimental 3
3.1 Test Materials 3
3.2 Solutions 3
3.2.1 Nitric Acid/Oxalic Acid Corrosion Testing. 3
3.2.2 Permanganate Test Solutions. 4
3.3 Test setup 5
3.3.1 Planned Interval Tests 5
3.3.2 Task 2 Electrochemical Testing 9
3.4 Test Procedure 14
3.5 Post-Test Characterization of Coupons 14
3.6 Data Analysis 15
4 Results and Discussion 15
4.1 Task 1 Data 15
4.1.1 Active electrode data 15
4.1.2 Passive coupon data 20
4.1.3 Corrosion rate of 304L stainless steel in spent acid solution. 23
4.1.4 Chemical Analysis. 24
4.1.5 Discussion and comparison of the active and passive data 25
4.2 Task 2: Electrochemical Corrosion Testing of Sodium Permanganate Cleaning Solutions with Sludge Simulants 26
4.2.1 Solution Chemistry and Preparation. 26
4.2.2 Open Circuit Potential Measurement 28
4.2.3 LPR and CPP results. 32
4.2.4 Cathodic polarization testing. 37
5 Conclusions 38
6 References 39

List of Figures

Figure 1. Electrochemical probe for tests: (a) end view and (b) side view. 7
Figure 2. Cell set-up for electrochemical tests. 8

Figure 3. Pourbaix Diagram for water. 10
Figure 4. Example CPP curve. 12
Figure 5. Cathodic region of a CPP curve showing the empirically determined E_h. 13
Figure 6. Open Circuit Measurements for the Active Electrodes in Each Test Solution. 16
Figure 7. Corrosion Rate for HM 20:1 Test Solution Calculated from the Linear Polarization Measurement. 17
Figure 8. Corrosion Rate for HM 50:1 Test Solution Calculated from the Linear Polarization Measurement. 17
Figure 9. Corrosion Rate for PUREX 20:1 Test Solution Calculated from the Linear Polarization Measurement. 18
Figure 10. Corrosion Rate for PUREX 50:1 Test Solution Calculated from the Linear Polarization Measurement. 18
Figure 11. Cyclic Potentiodynamic Polarization Curve for Test HM 50:1 taken at 2 Weeks. 19
Figure 12. Cyclic Potentiodynamic Polarization Curve for Test HM 50:1 taken at 4 Weeks. 20
Figure 13. Plot of the Corrosion Rate for Each Passive Coupon in Test HM 20:1 22
Figure 14. Plot of the Corrosion Rate for Each Passive Coupon in Test HM 50:1 22
Figure 15. Plot of the Corrosion Rate for Each Passive Coupon in Test PUREX 20:1. 23
Figure 16. Plot of the Corrosion Rate for Each Passive Coupon in Test PUREX 50:1. 23
Figure 17. Open Circuit Measurements of 10M NaOH: 0.05M $NaMnO_4$ Comparing a Newly Made Solution with an Aged Solution. 27
Figure 18. Frost Diagram for Mn at pH=0 (solid line) and pH=14 (dashed line).[10] 27
Figure 19. Pourbaix Diagram for Manganese with Annotations of the Colors of the Manganese Species in Aqueous Solution. 28
Figure 20. Open Circuit Potential Measurements vs. SCE for 10M NaOH: 0.05M $NaMnO_4$ Tests. 30
Figure 21. Open Circuit Potential Measurements vs. SCE for 5M NaOH: 0.05M NaMnO4 Tests. 30
Figure 22. Open Circuit Potential Measurements vs. SCE for 3M NaOH: 0.05M NaMnO4 Tests. 31
Figure 23. Open Circuit Potential Measurements vs. SCE for 0.18M HNO_3: 0.05M NaMnO4 Tests. 31
Figure 24. Photos of Electrodes Post Electrochemical Testing Using Sodium Permanganate. 34
Figure 25. Cyclic Potentiodynamic Polarization Plot of 10 M NaOH: 0.05 M $NaMnO_4$. 35
Figure 26. Cyclic Potentiodynamic Polarization Plot of 3 M NaOH: 0.05 M $NaMnO_4$ with HM Simulant. 35
Figure 27. Cyclic Potentiodynamic Polarization Plot of 0.18M HNO_3: 0.05 M $NaMnO_4$. 36
Figure 28. Cyclic Potentiodynamic Polarization Plot of 0.18 M HNO_3: 0.05 M NaMnO4 with PUREX Simulant. 36

List of Tables

Table 1. Test Matrix for Corrosion Testing of A285 in NA/OA Chemical Cleaning Solution 4
Table 2. Electrochemical Corrosion Test Matrix for Task 2. 5
Table 3. Planned Interval Coupon Test 6
Table 4. Coupon Measurements and Calculated Surface Areas. 7
Table 5. Intergrated and Maximum Corrosion Rates Calculated from the Linear Polarization Measurements. 19

Table 6. Corrosion Rates in Mils Per Year from Passive Exposure Coupons Determined by Weight Loss. 21
Table 7. Test results of the 304L Stainless Steel Exposure Tests on the Spent Acid Solutions. 24
Table 8. pH of Test Vessels During Testing. 24
Table 9. Analytical Results of the Samples Collected During Testing for Aluminum, Iron, and Mercury, in mg/L. 25
Table 10. Open Circuit Measurements for Tests Described in Table 2. 29
Table 11. General Corrosion Rates for Sodium Hydroxide and Nitric Acid Solutions with 0.05M $NaMnO_4$ Mixed in a 20:1 Ratio with the Test Simulants for ASTM A285 Carbon Steel Performed at Room Temperature (22ºC ± 2°C). 33
Table 12. Cathodic Polarization Parameters for Hydroxide and Nitric Acid Solution Testing. 37

Abbreviations

ASTM	American Society of Testing and Materials
BOAC	Bulk oxalic acid cleaning
CPP	Cyclic potentiodynamic polarization
CP	Cathodic polarization
DOE	Department of Energy
EM	Environmental Management
HLW	High level waste
HM	H-Modified; The enriched uranium process that recovers plutonium and enriched uranium from uranium-aluminum fuel
LPR	Linear polarization resistance
LTAD	Low Temperature Aluminum Dissolution
MPY	mils per year
NA	Nitric acid
OA	Oxalic acid
OCP	Open circuit potential
PAR	Princeton Applied Research
PUREX	Plutonium Uranium Reduction Extraction
SCE	Saturated calomel electrode
SRNL	Savannah River National Lab
SRS	Savannah River Site

1 Executive Summary

The testing presented in this report is in support of the investigation of the Alternative Chemical Cleaning program to aid in developing strategies and technologies to chemically clean radioactive High Level Waste tanks prior to tank closure. The data and conclusions presented here were the examination of the corrosion rates of A285 carbon steel and 304L stainless steel when interacted with the chemical cleaning solution composed of 0.18 M nitric acid and 0.5 wt. % oxalic acid. This solution has been proposed as a dissolution solution that would be used to remove the remaining hard heel portion of the sludge in the waste tanks. This solution was combined with the HM and PUREX simulated sludge with dilution ratios that represent the bulk oxalic cleaning process (20:1 ratio, acid solution to simulant) and the cumulative volume associated with multiple acid strikes (50:1 ratio). The testing was conducted over 28 days at 50℃ and deployed two methods to invest the corrosion conditions; passive weight loss coupon and an active electrochemical probe were used to collect data on the corrosion rate and material performance. In addition to investigating the chemical cleaning solutions, electrochemical corrosion testing was performed on acidic and basic solutions containing sodium permanganate at room temperature to explore the corrosion impacts if these solutions were to be implemented to retrieve remaining actinides that are currently in the sludge of the tank.

Based on passive coupon tests, the high acid to sludge ratio (50:1) results in a solution that is more corrosive than the low acid to sludge ratio (20:1). For example, the corrosion rates for the PUREX simulant at a 50:1 ratio ranged from approximately 250 to 490 MPY, whereas for the 20:1 ratio the rates ranged from approximately 120 to 240 MPY. A similar trend was observed for the HM simulant. Additionally, the dissolution of the PUREX sludge results in a simulant that is more corrosive than the solution that results from dissolution of the HM sludge.

Both dissolved sludge simulants resulted in similar trends in solution corrosivity and metal corrodibility. The ratio of acid to sludge determined the evolution of the solution corrosivity and metal corrodibility. For the 20:1 acid to sludge ratio, the solution corrosivity increases with time, whereas for the 50:1 ratio the solution corrosivity decreases with time. For both 20:1 and 50:1 sludge ratios, metal corrodibility increases with time. This suggests that the ferric oxalate film that forms on the steel surface degrades with time and offers less protection.

Corrosion rates from the passive coupon tests for the nitric acid/oxalic acid blend are significantly greater than those from the LPR measurements. There are several factors that could contribute to this. This result may be due to simultaneous electrochemical and chemical dissolution of the steel. As a result, the results from the LPR tests would not be useful without significant correction. Further testing would be necessary to determine if chemical dissolution were a factor.

The corrosion rate data from the coupon tests in the nitric acid/oxalic acid blend would need to be evaluated to determine the degree of potential structural damage. The corrosion rates, although relatively high, would not be expected to cause damage that would reduce the capacity of the tank primary if the process is completed within a month.[1] The OCP measurements do indicate that hydrogen evolution is thermodynamically possible. However, further studies would be needed to determine the rate at which hydrogen evolution occurs.

The corrosivity of sodium permanganate in four proposed cleaning solutions, 1 nitric acid solution and 3 sodium hydroxide solutions, was studied by electrochemical methods at room temperature. The corrosion rates were less aggressive than in the oxalic acid tests. The most aggressive solution was the 3M sodium hydroxide with permanganate which had corrosion rates greater than 20 mils per year based on linear polarization tests. The cyclic potentiodynamic polarization tests indicated that primarily general corrosion occurs. Passive coupon tests need to be performed in these solutions to ensure that chemical dissolution of the metal is not occurring simultaneously.

The following future activities are recommended for the corrosion phase of this program:

1. Perform potentiostatic tests in nitric/oxalic solutions to confirm and establish the degree to which chemical dissolution, as opposed to electrochemical corrosion, of the steel occurs.
2. Perform electrochemical tests on stainless steel exposed to permanganate solutions (caustic and acidic).
3. Perform electrochemical tests on carbon steel and stainless steel in permanganate solutions (caustic and acidic) at higher temperatures.
4. Perform 1 month coupon tests on carbon steel and stainless steel in permanganate solutions (caustic and acidic) at process temperature.

2 Background

The U. S. Department of Energy (DOE) Office of Environmental Management (EM) has tasked the Savannah River National Laboratory (SRNL) with developing strategies and technologies to chemically clean radioactive High Level Waste (HLW) tanks prior to tank closure.[2] Two tank cleaning technologies have already been implemented at the Savannah River Site (SRS): Low Temperature Aluminum Dissolution (LTAD) and Bulk Oxalic Acid Cleaning (BOAC). Recent chemical cleaning efforts on SRS Tank 12 were very successful with regard to sludge heel (especially for Al, Fe, and U phases) and beta/gamma radionuclide removal.[3] The Tank 12 chemical cleaning strategy utilized the following processing sequence: LTAD, washing, BOAC, and neutralization. Although chemical cleaning using these technologies has been shown to be effective, no disposition path has been identified for oxalate added during BOAC, and insoluble oxalate salts are accumulating within the SRS tank farm and waste processing facilities (e.g. evaporators).[4] Extensive sludge washing is also required to remove moderately soluble sodium oxalate salts prior to sludge vitrification in the SRS Defense Waste Processing Facility (DWPF).[4] As a result, oxalate additions to the tank farm need to be minimized by the use of supplementary acids to assist sludge removal in oxalic acid (OA) or the use of other cleaning reagents or processing strategies.

Previous SRNL testing[5-6] revealed the importance of pH control for BOAC, recommended the use of a supplementary acid (i.e. dilute HNO_3) with OA to minimize oxalate additions,[7] and indicated that marginal corrosion rates would be observed with these acid blends.[8] The heel pH was maintained to near the ideal value for sludge dissolution during BOAC (~pH 2) in SRS Tank 12, but a supplementary acid was not utilized.

Primary drivers in SRS Tank Closure Performance Assessments, which evaluate the fate and impact of tank sludge residuals on a geological timescale, are the removal of alpha emitting radionuclides present at low concentrations such as Pu, Am, and Np, which are not highly soluble in currently utilized chemical

cleaning reagents. Scoping studies conducted at SRNL revealed promising methods to dissolve the actinides within the HLW tank heels.[9] Oxidation of the actinides with permanganate in either strong caustic (i.e., 3, 5, and 10 M NaOH) or dilute acidic (i.e., 0.18 M HNO_3) solutions was shown to result in dissolution of oxy/hydroxide phases of these metals in the absence of major sludge phases. Either of these two permanganate-based methods for alpha removal might be suitable for incorporation into a chemical cleaning flow sheet, though they would likely be utilized at different times in the processing sequence. Utilization of permanganate-based methods results in the addition of manganese oxide solids to the waste, so minimization of permanganate additions is needed.

This report presents the results of the corrosion evaluation component of the Alternative Chemical Cleaning program. The corrosion evaluation was divided into two tasks. Task 1 focused on one month corrosion tests that included electrochemical probe measurements and passive, weight loss coupons to evaluate corrosion loss using the chemical cleaning solution along with sludge waste simulants at two dilution conditions. Task 2 is a corrosion screening test that concentrated on the corrodibility of sodium permanganate in the conditions that would be used for in-tank treatment of the sludge types of interest.

3 Experimental

3.1 Test Materials

American Society of Testing and Materials (ASTM) A285 carbon steel materials were utilized for the corrosion tests. The Type I and II SRS waste tanks, which are the initial tank groups targeted for chemical cleaning and closure, were constructed of A285 carbon steel. Immersion test coupons were sectioned from a plate of A285 material supplied by Metal Samples Company™ (Munford, AL). The coupons were polished to a 600 grit finish to provide a uniform, reproducible surface prior to testing. This surface preparation was utilized in the previous corrosion tests for the same purposes.[8]

The test material, 304L stainless steel, was also used for the corrosion tests. SRS tank farm transfer lines and ventilation system materials were constructed of 304L stainless steel. Immersion coupons were sectioned from a plate of 304L material also supplied by Metal Samples Company™. The coupons were polished to a 600 grit finish to provide a uniform, reproducible surface prior to testing.

3.2 Solutions

3.2.1 Nitric Acid/Oxalic Acid Corrosion Testing.

The cleaning solution utilized for these tests contained a mixture of 0.18 M nitric acid (NA) and 0.056 M (0.5 wt. %) oxalic acid (OA) based on previous recommendations for OA cleaning.[7] The test temperature was 50 °C and the two acid: sludge volume ratios tested were: 20:1 and 50:1. These ratios were assumed to simulate the multiple acid strikes (cumulative acid to sludge volume ratio 50:1) typically used for the waste tank chemical cleaning process and BOAC baseline (20:1).

The sequence for the addition was the following:

Step 1

- Add 0.18 M NA at ambient temperature to achieve a pH of 1 to 2 with temperature controls to avoid exceeding 50 ºC.
- Allow the system to equilibrate for 1 day.
- Remove the NA.

Step 2

- Add OA/NA blend at 50 ºC to the target acid: sludge volume ratio.
- Evaluate the samples over a period of 4 weeks.

Previous laboratory testing has also suggested that agitation results in higher general corrosion rates. Therefore, the simulants were agitated during the Steps 1 and 2.

Two sludge simulant formulations developed by Eibling[10] which are representative of SRS PUREX and HM sludge types were evaluated. These simulants were used during previous chemical cleaning corrosion testing.[8,10] The recipes were developed to simulate the dissolution characteristics of waste tank heels by the addition of portions of the major Fe and Al sludge components as oxide or hydroxide phases. The HM sludge slurry simulant recipe was developed based on SRS Tank 12 sludge samples obtained prior to aluminum dissolution operations. The sludge is comprised primarily of aluminum, iron, and manganese oxides and hydroxides with numerous of secondary metal oxides and hydroxides. In addition , the sludge simulant also included the hazardous metals Ag, Ba, Cd, Cr, Hg and Pb. The PUREX simulant compositional basis was developed from information on SRS Tank 8F sludge. The sludge is comprised primarily of iron and manganese oxides and hydroxides with numerous of secondary metal oxides and hydroxides, but also included Ag, Ba, Cd, Cr, Hg and Pb. Minor metal species present in these simulant formulations could have significant impacts upon the corrosivity toward steel. Table 1 shows the matrix of corrosion tests that were performed.

Table 1. Test Matrix for Corrosion Testing of A285 in NA/OA Chemical Cleaning Solution

	Acid/Sludge Slurry Ratio	
Type of Sludge	20:1	50:1
HM	X	X
PUREX	X	X

In order to simulate conditions in the waste transfer lines, tests on 304L stainless steel were conducted using spent acid solutions produced by the tests above. The vessels containing the acid and simulant were used without stirring leaving the coupons exposed to the spent acid solutions. The coupons were exposed to these NA/OA solutions for 4 weeks at a test temperature of 50 °C.

3.2.2 Permanganate Test Solutions.

Four test solutions were utilized:

1) 10 M sodium hydroxide / 0.05 M sodium permanganate
2) 5 M sodium hydroxide / 0.05 M sodium permanganate

3) 3 M sodium hydroxide / 0.05 M sodium permanganate
4) 0.18 M nitric acid / 0.05 M sodium permanganate

In addition to tests in these solutions, tests were performed in these solutions combined with the PUREX and HM simulants developed by Eibling.[10] These conditions will simulate the actual chemical cleaning process. Previous testing with oxalic acid has shown that the presence of the simulated sludge solids, and the associated interstitial liquid, affects the corrosion behavior of the carbon steel.[8] The liquid to solid phase ratios used for testing were 20:1. Tests were conducted at ambient temperature with temperature monitoring. In order to obtain better dissolution of the solids, the waste is typically agitated by pumps. Previous laboratory testing has also suggested that agitation results in higher general corrosion rates. Therefore, the simulants were agitated during the testing.[7]

Testing was performed utilizing A285 Grade C carbon steel electrodes. The test matrix is shown in Table 2.

Table 2. Electrochemical Corrosion Test Matrix for Task 2 in Caustic and Acidic Permanganate Solutions.

Test	Material	Sludge	Solution
1	A285	None	1
2	A285	None	2
3	A285	None	3
4	A285	None	4
5	A285	HM	1
6	A285	HM	2
7	A285	HM	3
8	A285	HM	4
9	A285	PUREX	1
10	A285	PUREX	2
11	A285	PUREX	3
12	A285	PUREX	4

3.3 Test setup

3.3.1 Planned Interval Tests

Changes in the solution corrosivity (i.e., aggressiveness of the environment) and alloy corrodibility (i.e., corrosion susceptibility, passive layer formation and/or degradation, etc.) can be determined with a planned interval testing program. The procedure for the program is illustrated in Table 3. In these tests, the waste simulants are contacted with the NA/OA cleaning reagent for a period of four weeks and steel coupons are immersed in this slurry for the intervals indicated. A minimum set of 3 flat, rectangular coupons with a surface area of 34.95 cm^2 (5.42 in^2) is initially exposed to the corrosive environment of interest. Duplicate or more sets may be included as well for statistical validity. Coupon #1 was removed after 1 week of exposure, coupon #2 was to be removed after 3 weeks of exposure, but was inadvertently removed after 2 weeks. Coupon #3 was removed after 4 weeks of exposure. Coupon #4, another flat, rectangular coupon, was placed in at 3 weeks and was removed along with Coupon #3 after week 4.

The analysis of the test results is also summarized in Table 3. A_1, A_3, and A_4 are the corrosion rates (general and/or pitting) obtained from Coupon numbers 1, 2 and 3, respectively. A_2 is the calculated difference in the corrosion rates between Coupon numbers 2 and 3. B is the corrosion rate obtained from coupon number 4. When $B=A_1$ the corrosivity of the environment has not changed after 3 weeks of exposure. On the other hand, if $B < A_1$ the corrosivity has decreased or if $B > A_1$ it has increased. Corrosion rate A_2 evaluates the corrodibility of the alloy. When $A_2 = B$ the alloy corrodibility has not changed after 3 weeks of exposure. In contrast, if $A_2 < B$ the corrodibility has decreased, and when $A_2 > B$ it has increased. However, since A_2 could not be calculated (due to the inadvertent removal of Coupon #2 at week 2), alloy corrodibility cannot be extrapolated from this test. Any combination of change in the environment corrosivity or alloy corrodibility is possible and can be obtained from planned interval testing.

Table 3. Planned Interval Coupon Test with NA/OA Chemical Cleaning Solution

Coupon					
	A1				
No.1					
		A3		A2	
No. 2					
				A4	
No. 3					
				B	
No. 4					
	1	**2**	**3**	**4**	
	Time(weeks)				

Criteria	**Environment Corrosiveness**	**Criteria**	**Alloy Corrodibility**
B = A1	**Unchanged**	**A2 = B**	Unchanged
B < A1	**Decreased**	**A2 < B**	Decreased
B > A1	**Increased**	**A2 > B**	Increased

In-situ monitoring of the corrosion during the test was performed with electrochemical probes. This technique has been utilized successfully to monitor corrosion processes in similar environments.[8] The electrochemical probes were prepared from the same A285 carbon steel material as the coupons. The pre-mounted probe was nominally 0.25" x 0.25" x 0.3" (i.e. 0.425 in^2 or 2.73 cm^2). However, the mounting of the electrodes was not always precise, so the area for each electrode was determined and recorded (see Table 4.) The surface areas of the individual electrodes were used in the corrosion calculations pertaining

to that electrode. The probe was prepared for testing by attaching a 22 AWG wire to one end of a coupon with silver epoxy. The probe was then mounted in a chemically resistant acrylic compound to protect the exposed end of the wire and the silver epoxy during the test and to provide an easily held sample (see Figure 1.)

Table 4. Coupon Electrode Dimensions and Calculated Surface Areas.

Sample ID	Length, in	Width, in	Height, in	Area in^2	Area cm^2
1	0.3655	0.3710	0.2375	0.5329	3.438
2	0.4655	0.3630	0.2365	0.6440	4.155
3	0.3921	0.3755	0.2385	0.5711	3.684
4	0.4310	0.3840	0.2360	0.6251	4.033
5	0.4409	0.3835	0.2365	0.6374	4.112
6	0.4195	0.3655	0.2355	0.5903	3.808
7	0.3454	0.3965	0.2320	0.5262	3.395
8	0.5401	0.3693	0.2317	0.7348	4.740

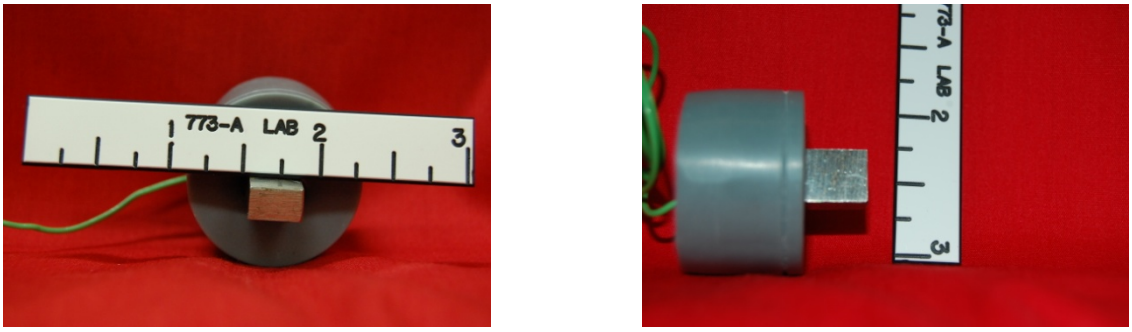

(a) (b)

Figure 1. Electrochemical probe for tests: (a) end view and (b) side view.

The tests with the electrochemical probes were performed concurrently with the coupon tests. To perform the corrosion measurements within each test vessel, an electrochemical cell was designed. The cell consisted of four primary features: a) a working electrode, b) a counter electrode, c) a reference electrode, and d) a potentiostat. Each feature is briefly described below.

The working, or corroding, electrode was the carbon steel probe. Two working electrodes were positioned in a glass “tree-like” holder for each test with the face oriented approximately perpendicular to the bottom of the vessel at about 2” and 4” from the bottom. The wires from the coupons were extended through the top of the vessel via a glass tube, where they were then attached to the potentiostat.

The counter electrode provided a path for an impressed current to flow through the solution from the working electrode. Materials that are conductive, yet chemically inert, are suitable for counter electrodes. In these tests carbon graphite rods were the counter electrodes. A 22 AWG wire was attached to one end of the rod with silver epoxy and covered with the acrylic mounting material. The counter electrodes were positioned to allow for a uniform current density to flow from the two working electrodes (see Figure 2). The working electrode pairs were numbered for each vessel; the odd electrode number is the upper electrode and even number is the lower electrode. Two carbon rods were oriented vertically in the vessel alongside the two electrodes to act as counter electrodes. The wires from the counter electrodes extended through the top of the vessel via the glass tube for connection to the potentiostat.

The reference electrode measures the electrochemical potential of a metal surface in a given environment. When a stable reference electrode is employed, any changes in the potential can be related to changes in the metal surface of the working electrode. These tests used a Radiometer XR-400 saturated silver/silver chloride (sat. Ag/AgCl) electrode. The reference electrode was held by a separate glass tube holder and fully immersed in the solution near the tree-like holder, away from the simulated sludge solids (see Figure 2). Typically it is desired to reduce the effect of the solution resistance on the measured potential by locating the reference electrode as close as possible to the working electrode. However, in this case the solutions were very conductive and the extended distance should not significantly impact the measured potential. The wire from the reference electrode extended through the top of the vessel via the glass tube for connection to the potentiostat.

The potentiostat consists of a power supply that applies the impressed current on the electrochemical cell and circuitry that measures and controls the potential to selected values.

The electrochemical measurements performed with the probes included: 1) Open circuit potential (OCP), 2) Linear polarization resistance (LPR), 3) Cyclic potentiodynamic polarization (CPP). A brief description of the relevance of the data and how the data will be collected is presented in the next section.

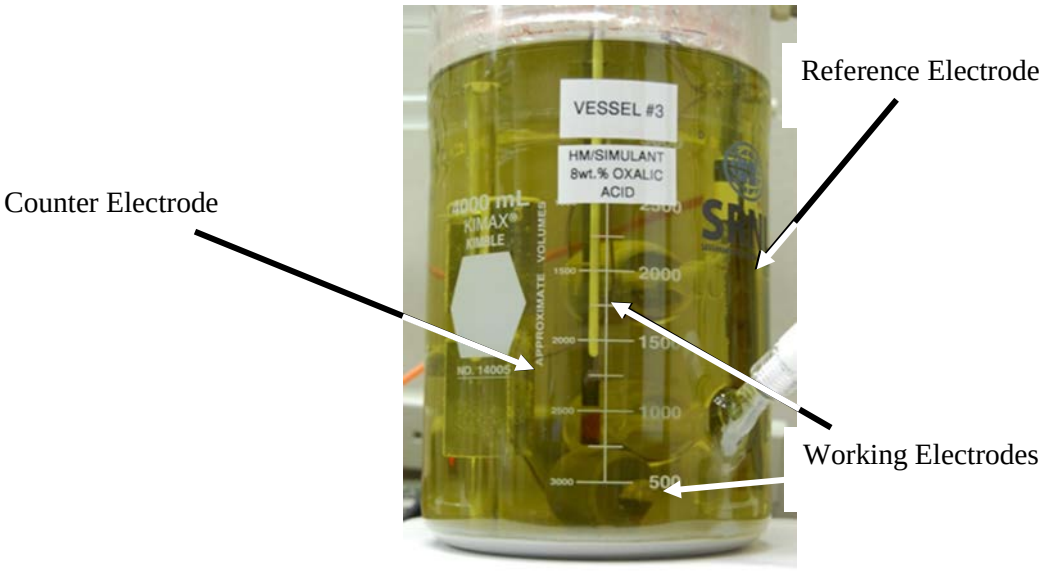

Figure 2. Cell set-up for electrochemical tests.

3.3.2 Electrochemical Testing

The electrochemical tests were conducted in a cell similar to the Princeton Applied Research (PAR) corrosion cell using a flat square electrode of A285 Grade C carbon steel embedded in epoxy with a flat exposed surface area of 3.629 cm^2. The electrode was connected by a piece 22 gauge wire that was spot welded to the sample before embedding. The sample was then polished to a 600-grit finish. After each set of measurements, the sample was resurfaced by wet polishing first with 240-grit sand paper, then 600-grit paper.

Four electrochemical tests were performed at each condition listed in Table 2. They are:

1) monitoring of the open-circuit potential (OCP),
2) linear polarization resistance testing (LPR),
3) cathodic polarization testing (CP), and
4) cyclic polarization testing (CPP).

In addition, between tests 2 and 3 and tests 3 and 4, the open circuit was monitored for 10 minutes. These tests were conducted with a PAR 273A potentiostat. Graphite rods were used as counter electrodes. In the first three tests with sodium hydroxide and sodium permanganate only, a $Ag/AgCl_2$ reference electrode was used, but the permanganate ion was observed to penetrate the electrode and appeared in the electrode solution. A luggin bridge was used with a saturated calomel electrode (SCE) to prevent continuous maintenance of reference electrodes and preserve data quality. The tests were measured with respect to the reference potentials.

The OCP reflects a measure of the activity at the metal surface for all oxidation and reduction reactions, i.e. whether it is actively corroding or passive, while the LPR testing will give a direct measure of the instantaneous corrosion rate. The cathodic polarization (CP) is performed to understand the nature of the cathodic reaction, while the cyclic potentiodynamic polarization (CPP) testing was performed separately to reveal any vulnerability to localized corrosion, such as stress corrosion cracking and/or pitting. The open circuit potential was measured during a 10-minute rest period between techniques to monitor for any significant changes during testing. These tests provide necessary mechanistic information to support the results of future coupon tests as well as screen for potential process conditions, which may result in lower corrosion rates. The conditions with lower corrosion rates could then be the focus of the coupon tests.

3.3.2.1 Open Circuit Potential

The OCP reflects a measure of the electrochemical activity at the metal surface, i.e. whether it is actively corroding or becoming passive. The test also provides information on the relative stability of the passive film, and whether hydrogen evolution is thermodynamically possible. For these tests, the OCP will be monitored daily to determine if changes in the passive film or environment may lead to a propensity for hydrogen evolution at any time during the test.

The propensity for hydrogen evolution may be visualized with the Pourbaix diagram for water, which is shown in Figure 3. The two diagonal lines, identified as (a) and (b), define the region of stability for water as a function of potential and pH. For potential and pH conditions between lines (a) and (b), water

is thermodynamically stable. For any value of potential above line (b), water is thermodynamically unstable and oxygen is liberated, while at any conditions of potential and pH below line (a), water is thermodynamically unstable and hydrogen gas is generated. Therefore, from the measured potential and the pH values, it can be determined if it is thermodynamically possible for the corrosion reaction to generate hydrogen. If the measured OCP value from the test is below line (a), hydrogen evolution is thermodynamically possible.

The equation for line (a) is derived from the Nernst Equation:

$$E_{H2} = E° - 2.303\frac{RT}{F} * pH \qquad (1)$$

where E_{H2} is the potential below which hydrogen evolution is thermodynamically stable, E° is the standard potential for hydrogen (E° = 0.0 V vs. NHE), R is the ideal gas constant, 8.314 J/mole-K, T is the temperature in K, and F is the Faraday constant, 96,500 J/equivalent. The potential utilized in the Nernst equation is with reference to the normal hydrogen electrode (NHE). Experimental measurements during these tests were made using a saturated Ag/AgCl reference electrode. To convert the potentials that are referenced to the hydrogen potential to one with reference to the Ag/AgCl, 197 mV are subtracted from E_{H2}. The potential below which hydrogen evolves can be determined as a function of pH and temperature.

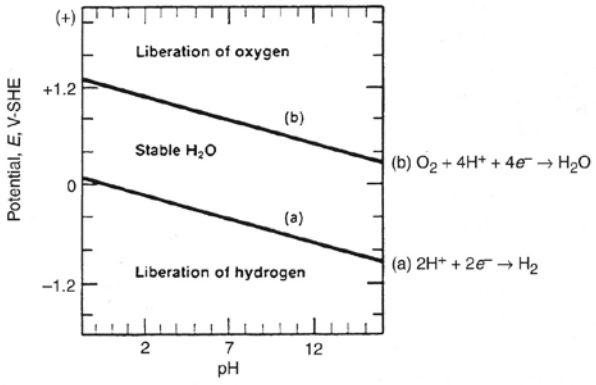

Figure 3. Pourbaix Diagram for water.

3.3.2.2 Linear Polarization Resistance

The linear polarization test will be performed in conjunction with the OCP monitoring. The LPR technique provides a non-destructive, instantaneous estimate of the uniform or general corrosion rate at a given specific time. In contrast, gravimetric (i.e., weight loss) measurements from coupons provide historical or integrated mass loss information from corrosion that has occurred over some period of time. The ASTM standard practice was utilized to conduct the test.[11] The technique is based on the observation that when the potential at the metal surface is polarized anodically or cathodically within 15 mV of the OCP, the measured current density at the metal surface increases linearly with potential. The slope of this line is defined as the polarization resistance (R_p). Stern and Geary modified the fundamental equation for

electrochemical reaction kinetics, and demonstrated that the relationship between the corrosion current density (i_{corr}) and R_p at the OCP is:

$$i_{corr} = \frac{\beta_a \beta_c}{2.3(\beta_a + \beta_c)R_p} \qquad (2)$$

where β_a and β_c are the anodic and cathodic Tafel slopes, respectively. If the Tafel slopes are unknown, frequently the assumed value for β_a and β_c is 0.120 V/decade. It has been shown experimentally that approximate values for β_a and β_c near 0.1 V/decade give a constant error in calculated corrosion rate of only a factor of two maximum. Such an error is frequently within experimental scatter for in plant corrosion measurements (i.e., typically gravimetric). Therefore, unless the actual slopes are quite different than 0.120 V/decade, the error in the value of i_{corr} is not significant.

Furthermore Stern states that i_{corr} measured by this technique differs from the actual corrosion rate by no more than a factor of two. In a more recent review Mansfield[12] showed from theoretical principles that the error in i_{corr} measurement is likely within ± 50% of the actual corrosion rate. Weight loss measurements for corrosion rates are typically reproducible to within 20 to 50%. Therefore, the inherent error in the corrosion rate measurement by either technique is similar.

The corrosion current density is related to the corrosion rate (CR) by the following equation:

$$CR = 0.13 * \frac{i_{corr} E_w}{\rho} \qquad (3)$$

where E_w is the equivalent weight of iron (27.9 g/equivalent), and ρ is the density of iron (7.86 g/cm^3). The corrosion rate is reported in mils (0.001 inches) per year.

3.3.2.3 Cyclic Potentiodynamic Polarization

Cyclic potentiodynamic polarization (CPP) will be the final electrochemical test performed. The CPP test will be initiated at a potential approximately 200 mV less than the E_{corr} at a given time. [Note: E_{corr} is the potential at which the rate of the anodic reaction equals the rate of the cathodic reaction. The value of E_{corr} depends on the kinetics of the anodic and cathodic half-cell reactions. For these tests, the value of E_{corr} is very close to the OCP.] A sequentially increasing potential will be applied to the probe at scan rate of 0.167 mV/s. The current response to the change in potential is measured to establish a current-potential relationship. At a potential approximately 1 V above the E_{corr}, the scan is reversed such that a sequentially decreasing potential is applied to the probe at the same scan rate. This test cannot typically be performed on the same probe within a matter of hours as may be done for the LPR test. That is because the degree of polarization needed for this test typically disturbs the metal surface of the probe so that a new surface is exposed. To obtain data at a later time in the test another probe is typically employed, or sufficient time is allowed for the sample to re-establish equilibrium. In these tests, CPP curves will be performed after 2 and 4 weeks of exposure. An example of a CPP curve from these tests is shown in Figure 4.

.

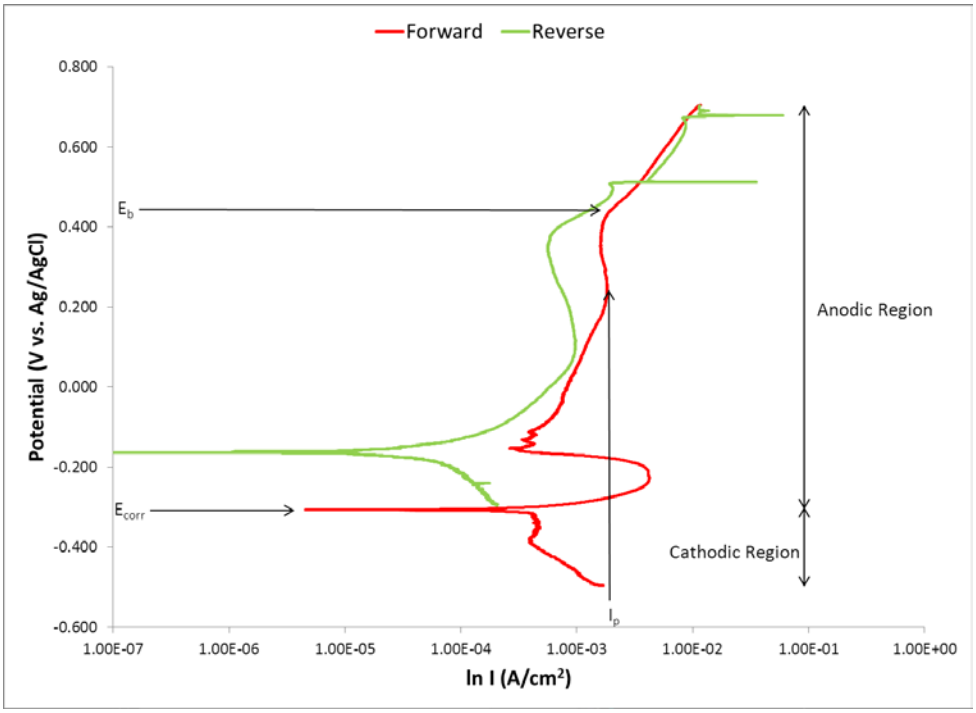

Figure 4. Example CPP curve.

The CPP curve will be utilized for three purposes. The first analysis involves the cathodic region of the CPP plot, which extends from E_{corr} to more negative potentials (see Figure 4). This region was used to investigate the kinetics of the cathodic electrochemical reaction. From these studies, the propensity for hydrogen may be investigated. At potentials relatively close to the E_{corr}, the relationship between the potential and the current is given by the Tafel expression

$$\eta = \beta \log (i/i_0) \qquad (4)$$

where η is the overvoltage, defined as $E - E_{corr}$, in volts; β is the slope of the line on the potential-log current density plot, also known as the cathodic Tafel slope in volts/decade of current; i is the measured current density at the applied potential E in A/cm^2; and i_o is the exchange current density, in A/cm^2, and represents the current density equivalent to the equal forward and reverse reactions at the electrode at equilibrium.

The dominant term controlling the corrosion rate for many metals exposed to non-oxidizing acids, such as oxalic acid, is hydrogen overvoltage at cathodic areas of the metal. Hydrogen overvoltage is the difference of potential between a cathode at which hydrogen is being evolved, and a hydrogen electrode at equilibrium in the same solution. The rate at which hydrogen evolution occurs depends on the catalytic properties of the electrode surface. A relatively pure iron corrodes at a low rate compared to a surface that contains impurities such as carbon, sulfur and phosphorous, which catalyze the hydrogen reaction.

To determine if hydrogen is the dominant cathodic reaction the following relationship was utilized:

$$\alpha = 2.3\ R\ T/(\beta\ F) \qquad (5)$$

where α is the transfer coefficient, R is the universal gas constant equal to 8.314 J/mole-K, T is the temperature in K, and F is the Faraday constant equal to 96,500 J /equivalent. For iron and steel, α is approximately 0.4 to 0.6 if the hydrogen reaction is occurring at the surface. If α is significantly less than 0.4, this is typical of a cathodic reaction that is diffusion controlled (i.e., β approaching infinite values). That is, the rate of cathodic reaction is dependent upon diffusion of the oxidizer to the electrode surface.

The cathodic region of the scan will be investigated to determine which reactions are possibly dominant. Of particular interest is the potential at which hydrogen evolution appears to be the clearly dominant cathodic reaction. This potential, defined as E_h, is determined empirically from the cathodic region of the CPP plot as shown in Figure 5. Below this potential the slope of the line on the potential-log current density plot is such that α from Equation 5 is approximately 0.4 to 0.6. For potentials at or below this value, hydrogen is the dominant cathodic reaction on the steel surface.

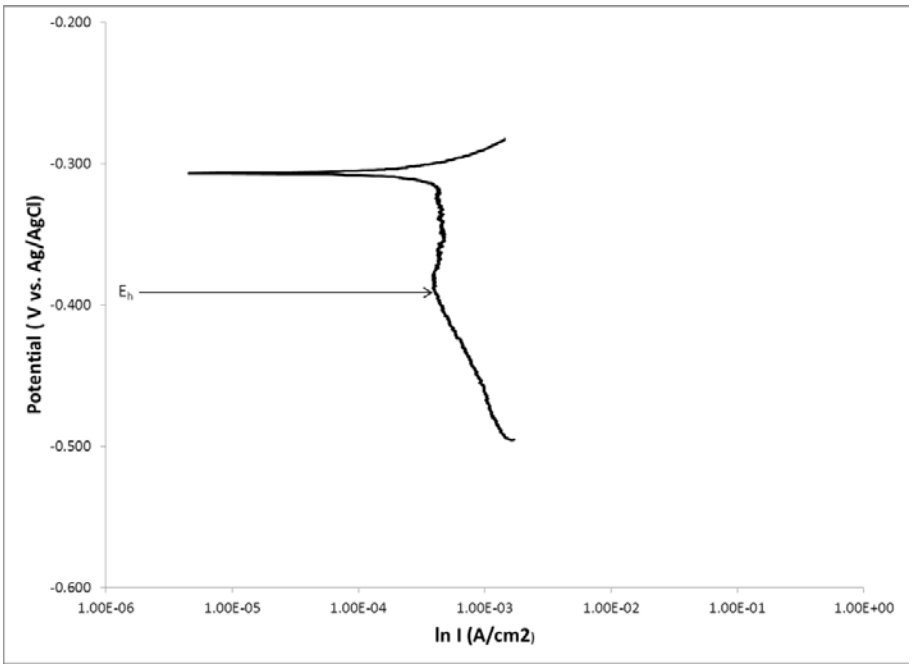

Figure 5. Cathodic region of a CPP curve showing the empirically determined E_h.

The anodic region of the CPP curve extends from E_{corr} to the more positive potentials of the forward scan. The current response provides mechanistic information on the metal dissolution or passivation reactions occurring at the metal surface. Current peaks are typically associated with metal dissolution and/or the oxidation of electro-active species in solution at the metal surface. Regions where the current is constant, and possibly low, are associated with passivation of the surface.

Various current responses that occur during the anodic or forward scan have been shown to be indicative of localized corrosion susceptibility. In particular, the breakdown potential, E_b, is the potential where the

current increases rapidly with a small change in potential. This change has been correlated with a reduction in the passive nature of the material. The passive to active transition region shown in Figure 4 is the region in which the material is susceptible to localized corrosion. The smaller the difference between values of E_{corr} and E_b, the more susceptible the material is to localized corrosion in that environment. The passive current density, I_p, is also indicative of the protective nature of the oxide film, or in this case the oxalate film. Lower passive current densities are indicative of a more stable protective film.

Data from the reverse scan as well as the forward scan are utilized to determine susceptibility to localized corrosion. If the current density of the reverse scan is greater than that for the forward scan, localized corrosion is likely. This behavior is known as positive hysteresis and indicates that pits have formed and are continuing to propagate. If the current density of the reverse scan is less than that for the forward scan, passive behavior is expected. This behavior is known as negative hysteresis and indicates that the passive film has re-formed on the surface.

3.3.2.4 Solution Analysis

Changes in the solution corrosivity were also monitored by obtaining periodic samples of the solution in Task 1. The samples were withdrawn in coordination with the removal of coupons; thus a correlation between constituents present in solution (e.g., aluminum) and the corrosion behavior may be drawn. That is, the following 3 samples were withdrawn:

1) Immediately after Coupon 1 was removed, 1 week.
2) Immediately after Coupon 2 was removed, 2 weeks.
3) Immediately after Coupons 3 and 4 had been removed, 4 weeks.

Non-rad ICP-ES was utilized to measure trends in the soluble concentrations of aluminum, iron, mercury, and other metals in solution.

3.4 Test Procedure

The electrochemical testing was performed using PAR 273A potentiostats and CorrWare control software. The linear polarization tests were done by performing a linear sweep of the potential from -0.25 mV to 0.25 mV with respect to the open circuit measurement at a scan rate of 0.166 mV/second. The CPP tests were performed by a linear sweep of the potential beginning at -0.250 V with respect to the open circuit potential at a scan rate of 0.166 mV/second to either a current limit (1.0 mA/cm^2) or a potential limit of 1.5 V vs. OCP. The CP test scanned from the OCP to -0.25 V vs. OCP at a rate of 0.166 mV/second.

3.5 Post-Test Characterization of Coupons

After testing, the passive coupons were treated with Clarke's solution to remove the corrosion products and determine the total weight loss due to corrosion processes in the experiment. The coupons were exposed for 3 minutes initially, then successively for 2 minutes. For the coupons that still had a high amount of corrosion products after 7 minutes of exposure, the coupons were exposed at 5-minute intervals. The coupon mass was recorded after each exposure. At the conclusion of the cleaning, the coupons were photographed. The final photographs will be assembled as an appendix to this report.

The corrosion rate was calculated in mils (millinches) per year (MPY) based on the mass loss in accordance with ASTM G 1-03.[13] The method calls to use the following equation:

$$\text{Corrosion Rate} = \frac{K \times W}{A \times T \times \rho}$$

Where, K is a conversion constant, 3.45×10^6, for MPY, W is the mass loss in grams, A is the surface area in cm^2, T is the exposure time in hours, and ρ is the density in grams/cm^3. The surface area of the corrosion coupons was determined to be 35.9504 cm^2.

3.6 Data Analysis

The instantaneous corrosion rates were determined from the polarization resistance measurements using CView software. The integrated corrosion rate was derived by integrating the plot of the instantaneous corrosion rate as a function of time then dividing the result by the total exposure time of 28 days, assuming a constant corrosion rate during the 28-day exposure. The integration was performed on the data points collected from the linear polarization tests which were imported into EC Lab® software to perform the mathematical integration. Data was collected and recorded in laboratory notebook SRNL-NB-2014-00037, "Corrosion Testing Experiments," and electronic notebook i7006-00164, "Corrosion Testing."

4 Results and Discussion

4.1 Task 1 Data

4.1.1 Active electrode data

The open circuit potentials were measured daily for the active probes in each vessel. Figure 6 shows the trend of the open circuit potentials for the duration of the testing for electrodes. It can be observed that the potential stays relatively negative and below -300 mV (vs. Ag/AgCl). In general, the potential remains relatively constant and there are only minor differences in the measured potential. The potentials are comparable to those for oxalic acid alone. Based on this data, hydrogen evolution is thermodynamically possible as the potential is less than that for hydrogen evolution.[8] Cathodic polarization studies would be needed to study the kinetics of the cathodic reaction to determine the rate of hydrogen evolution.

In addition, a linear polarization resistance measurement was collected daily from which the corrosion rate could be calculated. Figure 7 through Figure 10 compare the corrosion rates measured from the LPR tests. The corrosion rates changed throughout the testing. In Figure 7, the HM 20:1 test shows the corrosion rate rose to a maximum after 12 days of testing, settling then around 100-120 MPY before decreasing to 50 MPY at the end of the testing. This behavior is similar to the PUREX 20:1 in Figure 9 where the corrosion rate increases from about an average of 50 MPY, peaks around 90 to 115 MPY then gradually decreases to the 40 to 60 MPY range at the end of the experiment. From Figure 8, the HM 50:1 corrosion rates exhibit a greater disparity between the electrodes. Electrode 3 shows a downward trend in the corrosion rates as the rate begins at 55 MPY and decreases to around 33 MPY at the end of the testing. Electrode 4, however, show more aggressive corrosion rates in the third quarter of the testing, but had a

similar decreasing trend at the end of the testing. The PUREX 50:1 test results, shown in Figure 10, exhibit a decline in the corrosion rate that is somewhat progressive. The corrosion rate appears to decrease steadily from around 150 MPY in the early stages of testing to about 55 MPY at day 12. Around day 15, the rate decreases again and remains steady around 40 MPY and then drops to below 30 MPY at the end of testing.

The integrated corrosion rate was calculated by integrating the daily measured instantaneous corrosion rates and dividing by the duration of the test. The results are presented in Table 5, along with the maximum corrosion measured during the testing. The 4-week integrated corrosion rate can be compared to the corrosion rate for the coupons that were exposed for 4 weeks (see Table 6).

All the electrodes experienced some build-up of sludge on the electrode surface during the testing. This could account for the steady decrease in corrosion rate, and for the increase of corrosion rate when the weight loss coupons were removed or put into place on days 8, 12, and 22. Another minor contribution to the decrease in corrosion weight may be the slow reduction in surface area of the coupon, as the corrosion rate is determined with consideration of the initial surface area of coupon.

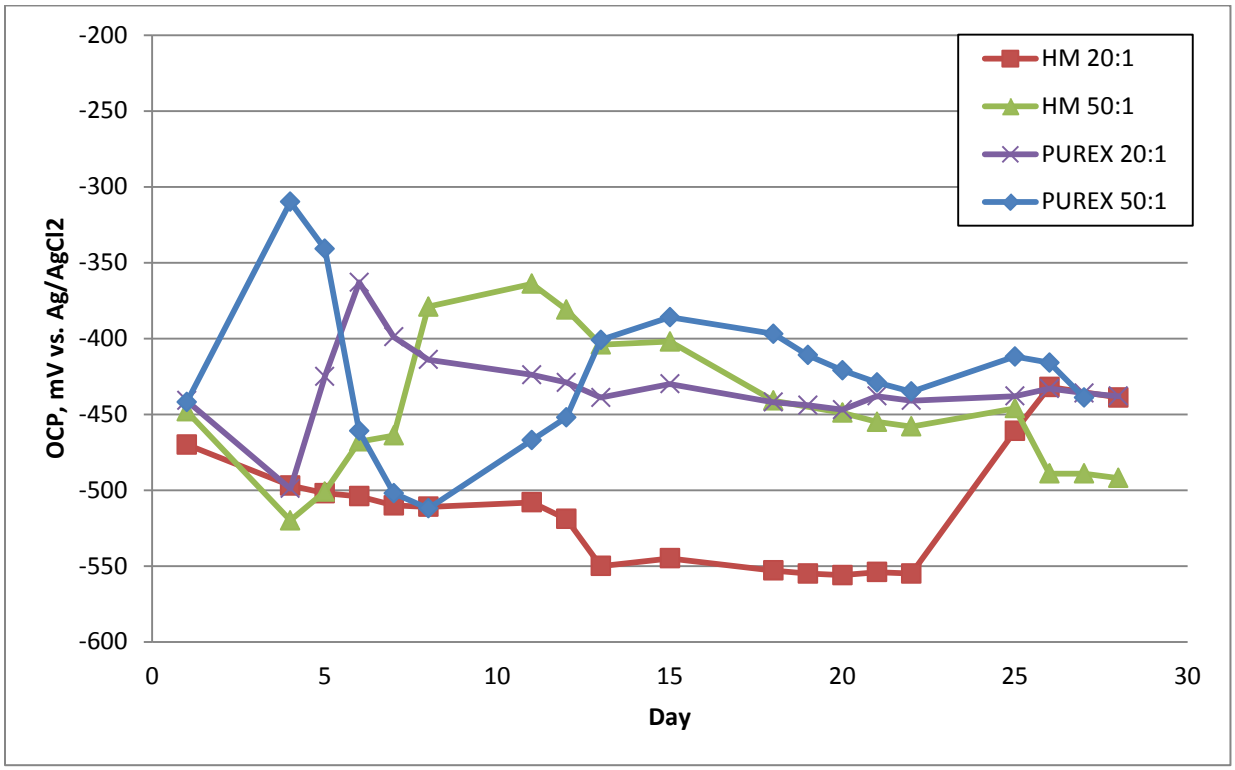

Figure 6. Open Circuit Measurements for the Active Electrodes in Each Test Solution.

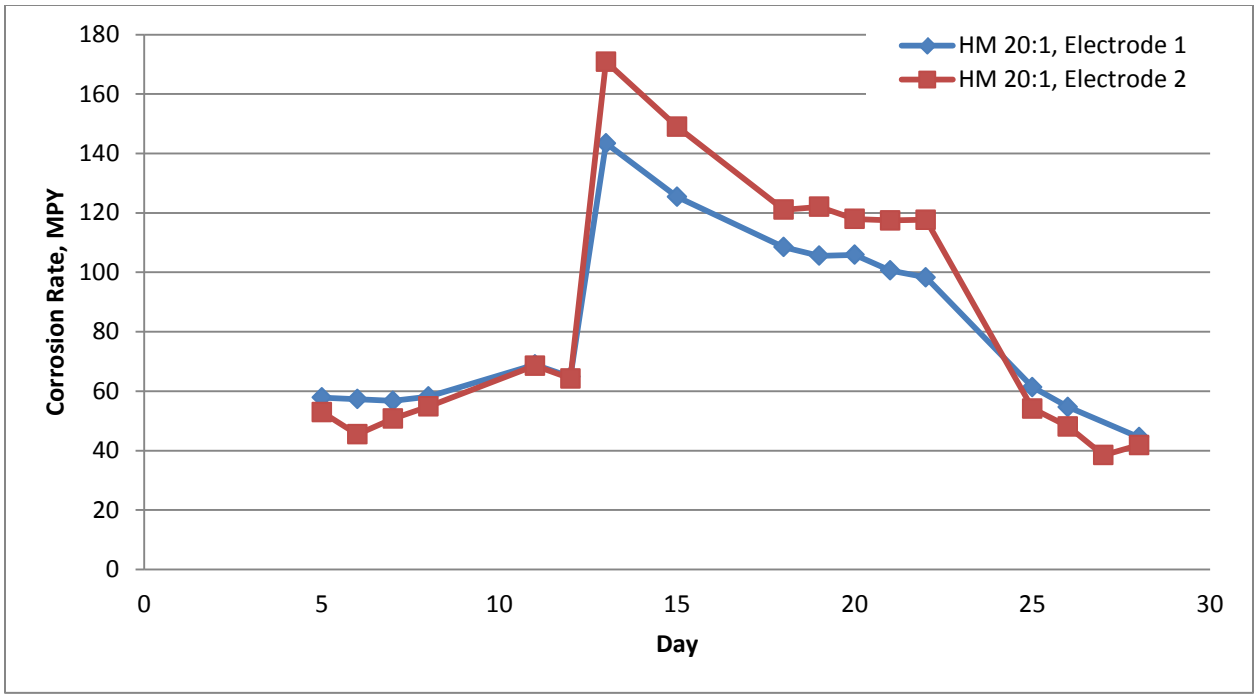

Figure 7. Corrosion Rate for HM 20:1 Test Solution Calculated from the Linear Polarization Measurement.

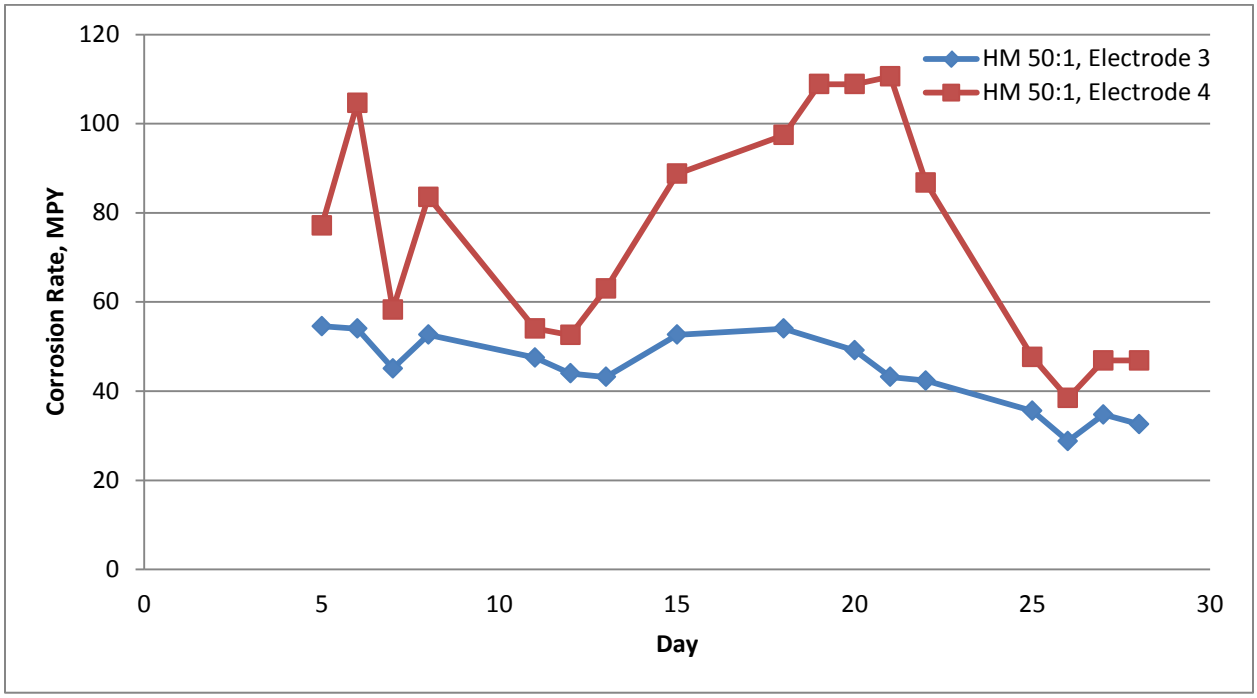

Figure 8. Corrosion Rate for HM 50:1 Test Solution Calculated from the Linear Polarization Measurement.

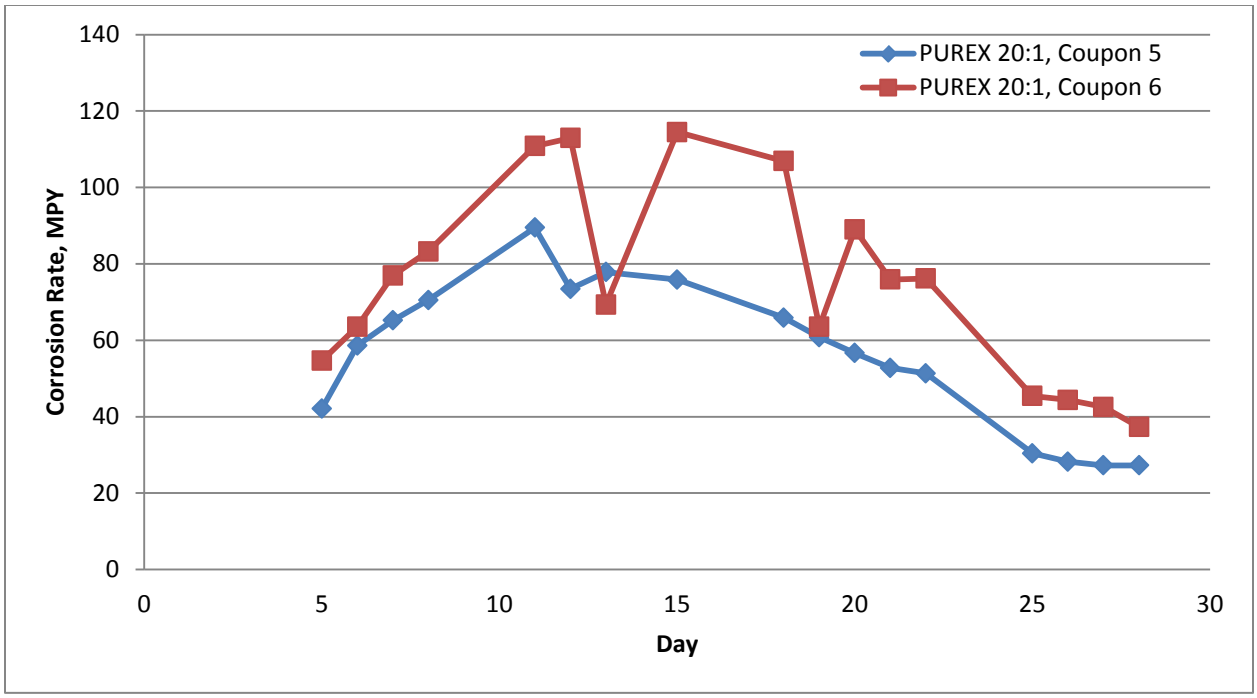

Figure 9. Corrosion Rate for PUREX 20:1 Test Solution Calculated from the Linear Polarization Measurement.

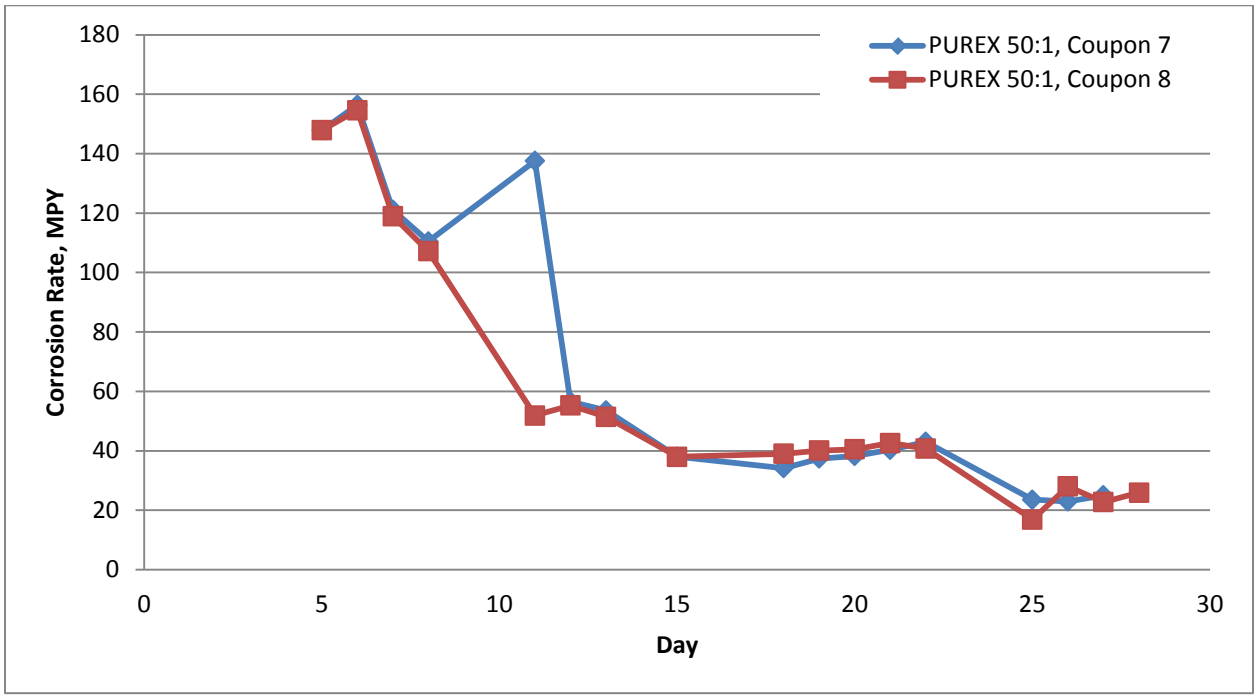

Figure 10. Corrosion Rate for PUREX 50:1 Test Solution Calculated from the Linear Polarization Measurement.

Table 5. Integrated and Maximum Corrosion Rates Calculated from the Linear Polarization Measurements.

	Electrode	Maximum Measured Corrosion Rate, MPY	Integrated Corrosion Rate, MPY
HM 20:1	1	143	70.2
	2	171	75.7
HM 50:1	3	111	36.5
	4	55	62.2
PUREX 20:1	5	114	49.3
	6	89	65.9
PUREX 50:1	7	156	52.0
	8	155	45.7

Cyclic potentiodynamic polarization tests were run on the active electrodes at the midpoint (2 weeks) and the conclusion of the testing (4 weeks). Two CPP plots are shown in Figure 11 and Figure 12 and are similar to the other plots collected in the tests insofar as active corrosion is observed. All of the CPP tests showed the characteristics that would indicate active corrosion is taking place (i.e., no passivation of the surface occurred).

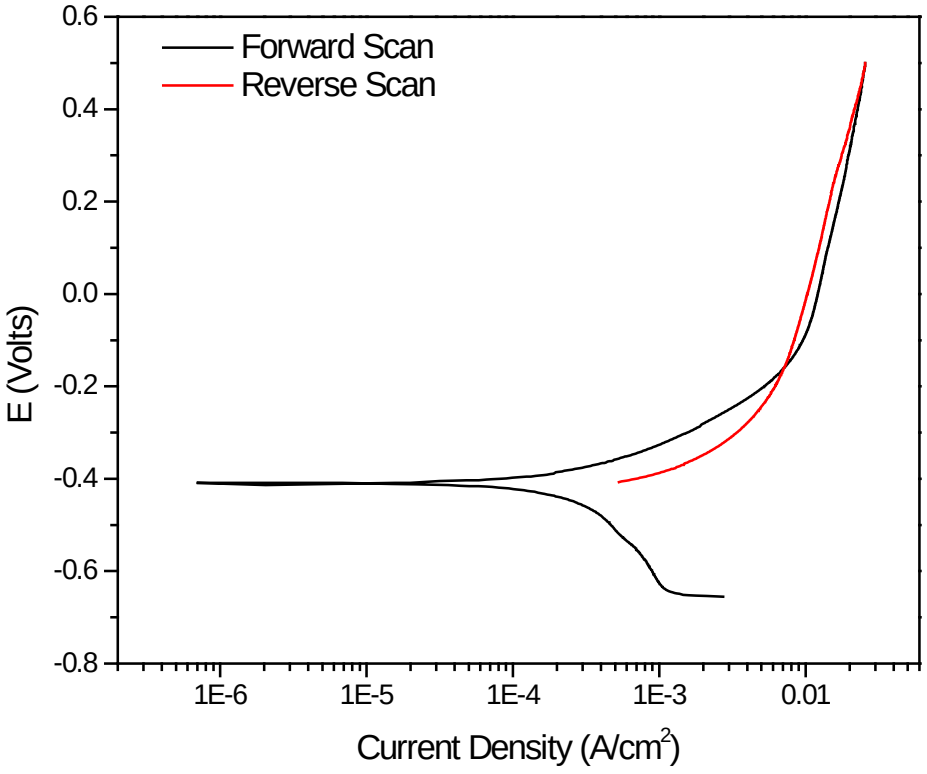

Figure 11. Cyclic Potentiodynamic Polarization Curve for Test HM 50:1 taken at 2 Weeks.

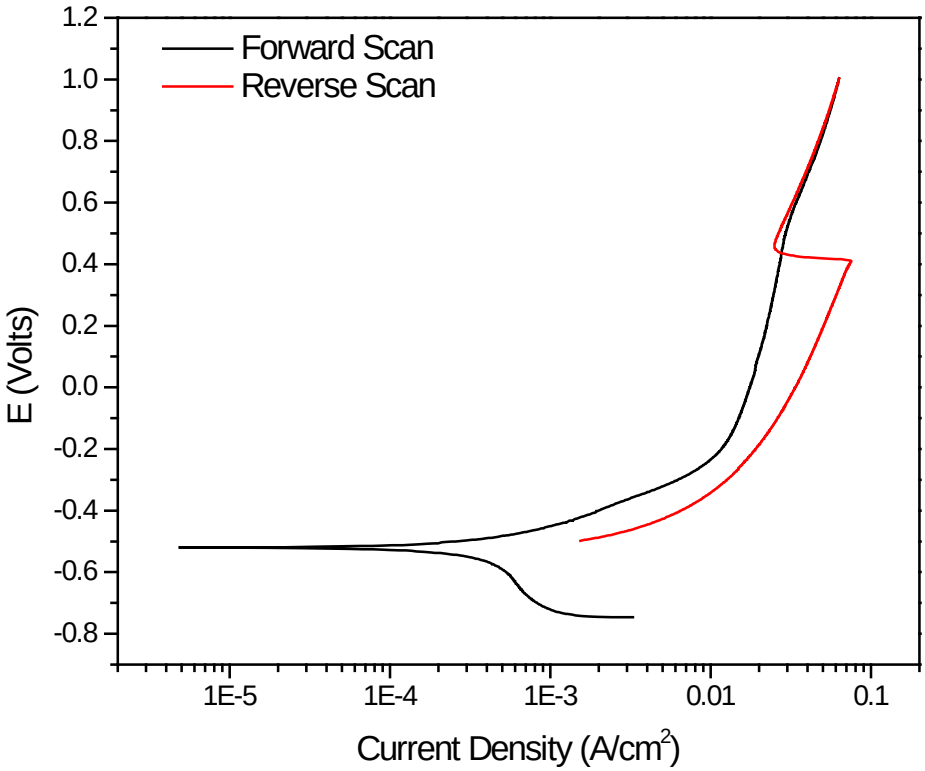

Figure 12. Cyclic Potentiodynamic Polarization Curve for Test HM 50:1 taken at 4 Weeks.

4.1.2 Passive coupon data

The data presented in Table 6 are the results of the weight loss measurements from the passive corrosion coupons that were exposed to the testing solutions. The corrosion rates are also presented in Figures 13 through 16. The first 3 coupons were exposed for 1, 2, and 4 weeks, respectively. The corrosion rates exhibited the following general trends. The 4 week coupon test data can be compared with the integrated corrosion rate data shown in Table 5. The dissolution of the PUREX sludge in NA/OA results in a simulant that is more corrosive than the solution that results from dissolution of the HM sludge. Corrosion rates for the PUREX simulants ranged from approximately 115 to 490 MPY, while for the HM simulants, the rates ranged from approximately 75 to 330 MPY. It should be noted that the corrosion rates for coupons 2 and 3 for the HM 50:1 were likely influenced by an adjustment that was made during the test. This test solution had a pH that was higher than expected after the first week of testing. At the time, 1 liter of acid solution was removed from the vessel and replaced with a new liter of solution. This step brought the pH back into alignment with the pH expectations for the testing. However, this likely increased the corrosion rates that were measured for coupons 2 and 3. If this is the case, for all comparable test conditions, the corrosion rates were higher in the PUREX simulants.

The high acid to sludge ratio (50:1) results in a solution that is more corrosive than the low acid to sludge ratio (20:1). For example, the corrosion rates for the PUREX simulant at a 50:1 ratio ranged from approximately 250 to 490 MPY, whereas for the 20:1 ratio the rates ranged from approximately 120 to 240 MPY. A similar trend was observed for the HM simulant. As will be shown later in Table 8, the pH

of the 50:1 simulants is generally lower than that for the 20:1 simulants. Table 9 also shows that the concentration of aggressive iron species (i.e., most likely the ferric oxalate species) is much greater in the 50:1 simulants than in the 20:1 simulants. Both of these observations corroborate the conclusion that the 50:1 ratio simulant produces a more corrosive solution than the 20:1 ratio simulant.

Table 6. Corrosion Rates in Mils Per Year from Passive Exposure Coupons Determined by Weight Loss.

Coupon	Time (hrs)	HM 20:1	HM 50:1	PUREX 20:1	PUREX 50:1
1	168	152.3	265.2	240.2	486.0
2	384	75.8	327.9	115.7	248.9
3	672	162.1	159.2	156.1	310.4
4	168	233.3	138.6	232.6	159.9

The corrosion rates from the first three coupons in combination with the corrosion rate from the fourth coupon can be used to assess the change in corrosivity of the solution and the metal corrodibility with time. The planned interval analysis described in section 3.3.1 revealed the following general trends. Both dissolved sludge simulants resulted in similar trends in solution corrosivity and metal corrodibility. The ratio of acid to sludge determined the evolution of the solution corrosivity and metal corrodibility.

For the 20:1 acid to sludge ratio, the solution corrosivity increases with time, whereas for the 50:1 ratio the solution corrosivity decreases with time. From Table 8, the pH for the solution remains relatively constant, and in addition the ferric ion concentration (see Table 9) increases. The result would be a solution that becomes slightly more corrosive with time. On the other hand for the 50:1 sludge ratio, the pH increases with time. Thus, despite an increase in the ferric ion concentration, the solution corrosivity decreases as the pH rises.

For both 20:1 and 50:1 sludge ratios, metal corrodibility increases with time. This suggests that the ferric oxalate film that forms on the steel surface degrades with time and offers less protection. This result correlates with previous tests that showed that at temperatures near 50 ºC, the ferric oxalate film that forms is loosely adherent to the metal surface.[8]

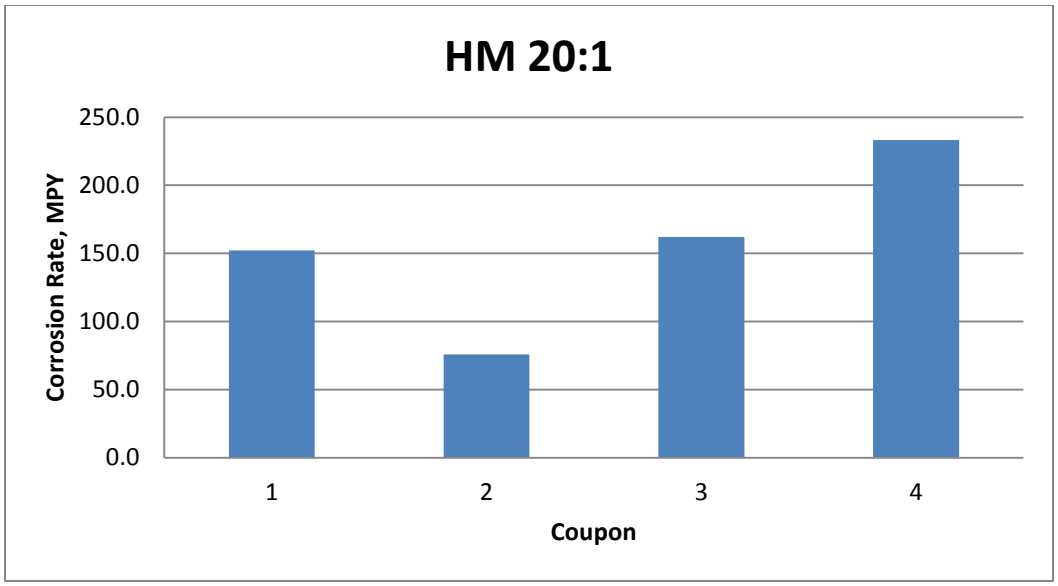

Figure 13. Plot of the Corrosion Rate for Each Passive Coupon in Test HM 20:1.

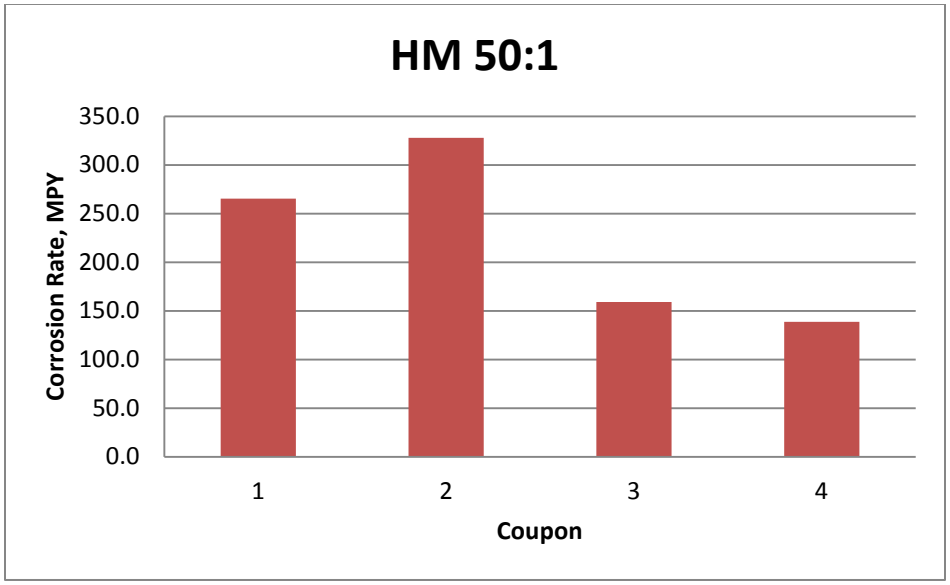

Figure 14. Plot of the Corrosion Rate for Each Passive Coupon in Test HM 50:1.

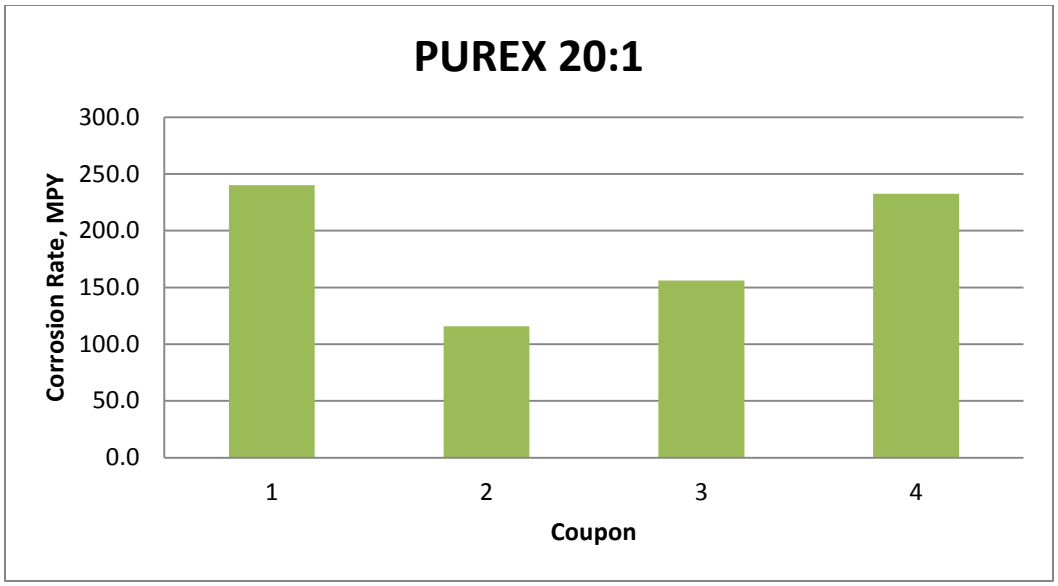

Figure 15. Plot of the Corrosion Rate for Each Passive Coupon in Test PUREX 20:1.

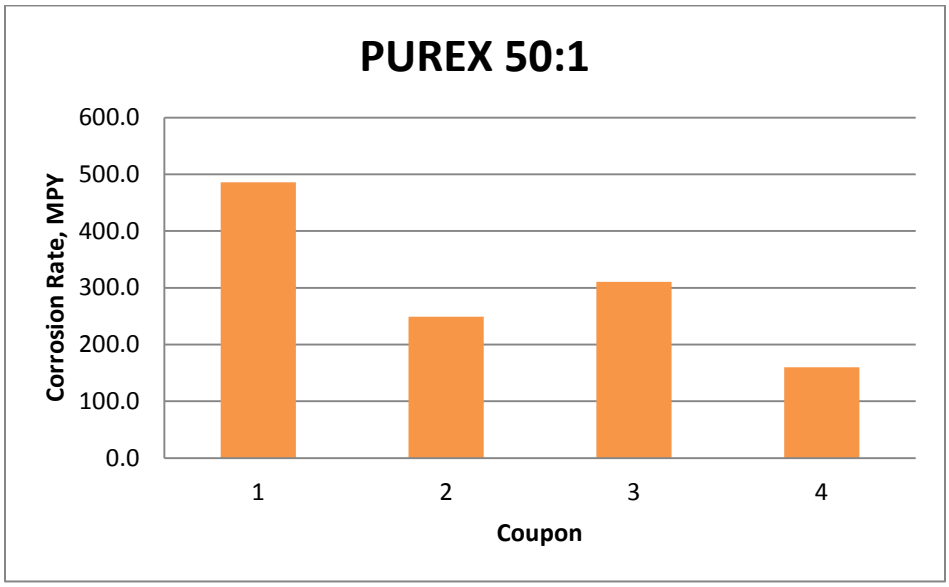

Figure 16. Plot of the Corrosion Rate for Each Passive Coupon in Test PUREX 50:1.

4.1.3 Corrosion rate of 304L stainless steel in spent acid solution.

The stainless steel tests yielded little to no corrosion for the exposure tests of 2 and 4 weeks. The results are presented in Table 7. The corrosion rates determined by weight loss were negligible with the highest corrosion rate being 0.2 MPY.

Table 7. Test results of the 304L Stainless Steel Exposure Tests on the Spent Acid Solutions.

	Coupon	Time (hrs)	Mass Loss(g)	Corrosion Rate, (MPY)
HM 20:1	1	384	0.002	0.1
HM 20:1	2	672	0.0014	0.0
HM 50:1	1	384	0.0022	0.1
HM 50:1	2	672	0.0018	0.0
PUREX 20: 1	1	384	0.0025	0.1
PUREX 20: 1	2	672	0.0031	0.1
PUREX 50:1	1	384	0.0041	0.2
PUREX 50:1	2	672	0.0038	0.1

4.1.4 Chemical Analysis.

The pH of the sludge simulant was adjusted using 0.18 M nitric acid to a pH range of 1 to 2 before the sludge was added to the nitric acid: oxalic acid cleaning solution. After the first week, it was noted that the HM 50:1 simulant was higher than expected and 1 liter of the acid solution was withdrawn from the vessel and replaced with 1 liter of new acid solution. Table 8 shows the pH values measured throughout the testing. The pH did not remain below pH 2 for any sample. Fluctuations were observed throughout the testing. The PUREX 50:1 solution showed the greatest pH increase, which as mentioned above resulted in a solution that became less corrosive with time. This solution had the lowest initial pH and the highest initial corrosion rate.

Table 8. pH of Test Vessels During Testing.

	HM 20:1	HM 50:1	PUREX 20:1	PUREX 50:1
Day 3	3.12	3.29	3.56	1.92
Day6	2.83	3.36	3.23	1.75
Day7	3.08	2.35*	3.49	2.31
Day 12	3.08	2.37	3.3	3.04
Day 21	3.02	2.55	3.23	2.8
Day 28	3.52	2.7	3.39	3.28

*Measurement after replaced acid.

The quantities of aluminum, iron, and mercury that dissolved in the simulants are presented in Table 9. The complete analysis is attached as Appendix B to this report. For both sludge simulants, greater quantities of iron were observed in the 50:1 acid to sludge ratio than the 20:1 sludge ratio. This correlates with the higher corrosion rates observed at the higher ratios. For both ratios, the concentration of iron increases with time and appears to be approaching a maximum concentration, particularly in the case of the 50:1 ratio. It is expected that as the iron concentration approaches a maximum, that this is an indication that the dissolution rate of the sludge has decreased, and the pH of the solution has increased. Thus, the corrosivity of the solution would be expected to decrease.

As expected based on the initial chemical composition of the sludge simulants, the amount of dissolved aluminum is higher for the HM sludge than the PUREX sludge. However, for both cases the dissolved aluminum decreases with time. Previous XRD analysis of solids from the metal surface taken from coupons exposed to oxalic acid and a sludge simulant have shown a build-up of aluminum oxides on the surface.[8] Thus, some precipitation of the aluminum from the solution may be occurring with time. A similar general trend was observed for Hg. In this case as well, elemental Hg was also observed on the surface of coupons that were exposed to oxalic acid. The presence of Hg on the surface disrupted the ferrous oxalate film.[8] Thus, these results appear to corroborate the general decrease in the metal corrodibility that was observed for the coupons.

Table 9. Analytical Results of the Samples Collected During Testing for Aluminum, Iron, and Mercury, in mg/L.

	Al	Fe	Hg
HM 20:1	**mg/L**	**mg/L**	**mg/L**
Week 1	1540.17	53.17	33.48
Week 2	993.59	914.66	17.23
Week 4	634.40	1425.00	9.52
HM 50:1			
Week 1	787.33	115.25	8.96
Week 2	610.91	2875.00	14.41
Week 4	616.50	2760.00	11.80
PUREX 50:1			
Week 1	1205.00	207.77	60.17
Week 2	968.25	2140.00	5.01
Week 4	755.03	2170.00	5.34
PUREX 20:1			
Week 1	513.66	318.19	34.17
Week 2	413.77	1435.00	1.09
Week 4	338.61	1525.00	<1.00

4.1.5 Discussion and comparison of the active and passive data

Overall, there is a discrepancy with the corrosion rates from the passive coupons and the corrosion rates measured by LPR. In general, the corrosion rates from the passive coupons are 2-6 times greater than those measured by LPR. This phenomenon has been observed for iron, chromium, and their alloys in acidic media.[12] Examples of this occurrence include: 1) iron in sulfuric acid that contains additions of potassium chromate, 2) stainless steel in hydrofluoric-nitric acid solutions, and 3) an iron-chromium alloy in sulfuric acid containing hydrogen peroxide.[14] In these cases, metal dissolution occurs not only by an electrochemical mechanism, but in parallel with a chemical mechanism. No current is passed by the chemical dissolution mechanism and hence the LPR measurements would underestimate the actual weight loss. Thus electrochemical measurements cannot be utilized to determine corrosion rates without major corrections. One commonality of these environments is that a reducing acid is in the presence of a strong oxidizer. In the present case, oxalic acid is a reducing acid and nitric acid is a strong oxidizer. Additional tests (i.e., potentiostatic and potentiodynamic) would need to be performed to confirm the chemical mechanism, but the discrepancy between the coupon and LPR results suggests that this is a possibility.

This observation has ramifications for both structural and flammability analysis. The OCP data suggests that hydrogen evolution is possible. However, due to chemical dissolution of the material, the hydrogen evolution rate may not be as high as predicted by the corrosion rates measured by the coupons. On the other hand, structural damage would likely exceed anticipated values if the corrosion rates from the LPR tests were accepted. Based on the present data, the corrosion rates from the coupon tests should be utilized for structural evaluations, while further kinetic studies are needed to evaluate hydrogen evolution.

4.2 Task 2: Electrochemical Corrosion Testing of Sodium Permanganate Cleaning Solutions with Sludge Simulants

4.2.1 Solution Chemistry and Preparation.

The introduction of the sodium permanganate in the high alkaline solutions, particularly the 10 M and 5 M NaOH, produced emerald green and blue solutions, respectively. These solutions were more viscous (thick) than the other solutions tested. The sodium permanganate was added from a 40% w/w stock solution. The stock solution was dark purple in color. When added to these hydroxide solutions, the permanganate ion slowly reduced from a Mn^{7+} to Mn^{6+}. This was observed by a color change from the deep purple to emerald green over time. When left over night, the 10 M NaOH solution stabilized as the emerald green color, whereas the 5 M NaOH stabilized as a dark blue color. Upon dilution, the blue color would change back to the purple permanganate, or if exposed to air, such as in a droplet, it would change to the emerald green color. It is presumed that a transient Mn^{5+} species is responsible for the blue color.[15] Both solutions returned to the purple color associated with Mn^{7+} when the solution was acidified whether with distilled water or acid. This suggests the oxidation state changes are due to the pH of liquid. The OCP of the 10 M NaOH: 0.05M $NaMnO_4$ was measured within an hour of adding the sodium permanganate solution and after aging for at least 24 hours. The OCP of the new (purple) solution had an OCP of 411 mV vs. $Ag/AgCl_2$ and was still decreasing after an hour. The aged solution (emerald green) had an OCP around 200 mV vs. Ag/AgCl as shown in Figure 17. The Frost diagram in Figure 18 suggests a decrease in potential that accompanies the oxidation state change from Mn^{7+} to Mn^{6+} at pH= 14. The 10 M NaOH solution should theoretically be pH= 15.[a] The Pourbaix diagram in Figure 19 also confirms that a reduction of potential would be accompanied with a change in oxidation state.

[a] pH = log ([OH]) + 14, at 10M, pH = log (10) + 14 = 15

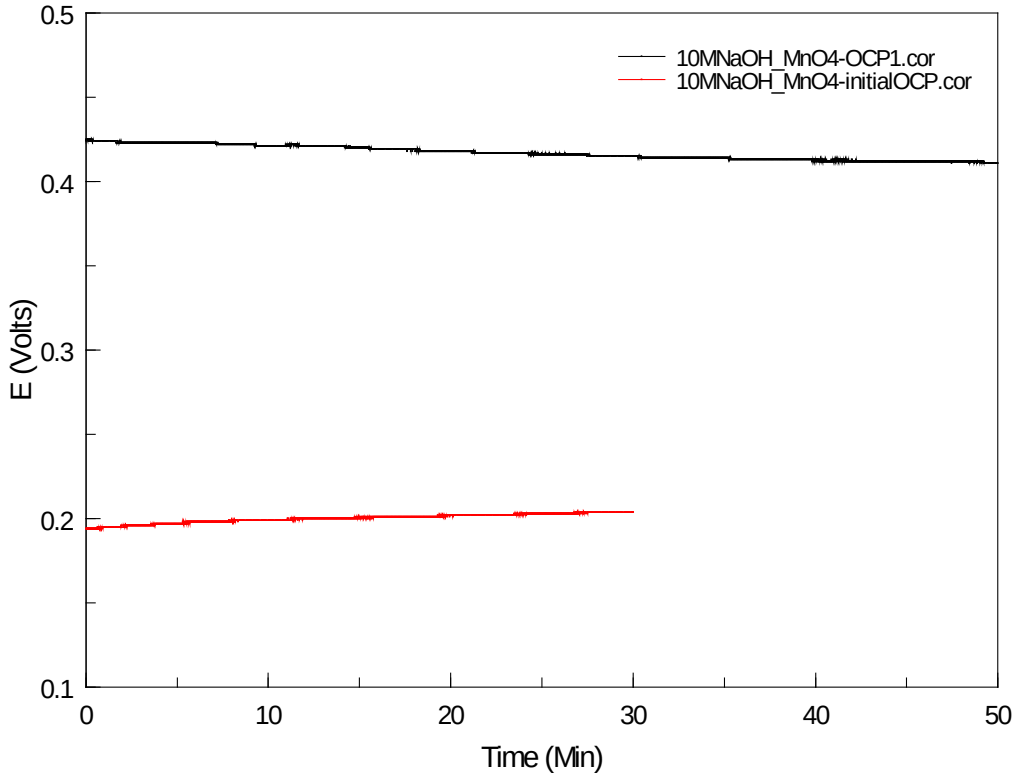

Figure 17. Open Circuit Measurements of 10 M NaOH: 0.05 M $NaMnO_4$ Comparing a Newly Made Solution (black) with an Aged Solution (red).

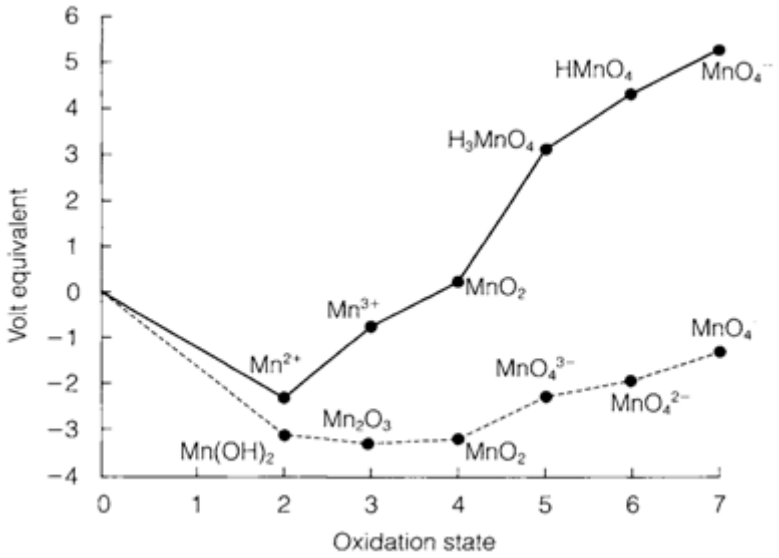

Figure 18. Frost Diagram for Mn at pH=0 (solid line) and pH=14 (dashed line).[10]

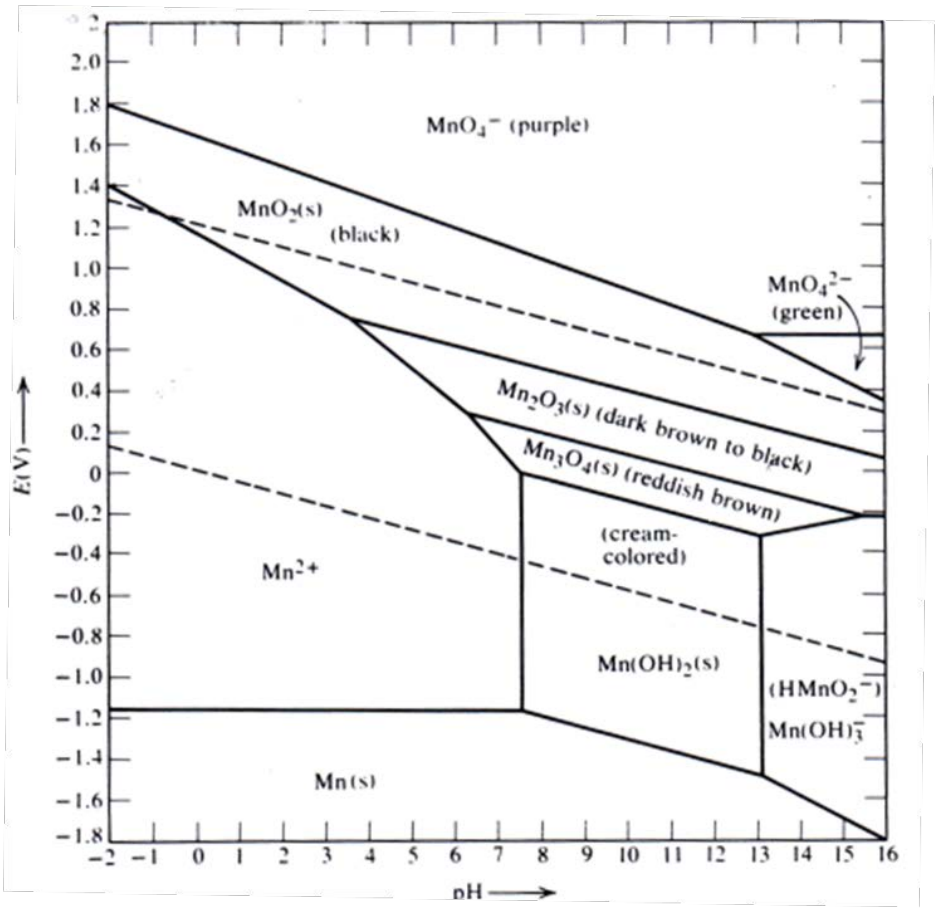

Figure 19. Pourbaix Diagram for Manganese with Annotations of the Colors of the Manganese Species in Aqueous Solution.

Little was found on the blue manganite ion, Mn^{5+}, which appeared in the 5M NaOH solutions, other than a discussion of the color.[15] The 5M NaOH solutions were allowed to age overnight before testing and the color was dependent on whether the container was open to the air or capped. If the container was capped, the solution would remain emerald green until it was poured into the electrochemical test cell then it turned to the blue color. However, drops on the edges of the cell and incidental spills would appear green and quickly oxidize on laboratory wipes to brown then appear to bleach the wipe.

4.2.2 Open Circuit Potential Measurement

Table 10 shows the results of the OCP measurements with respect to the saturated calomel reference electrode (SCE). Each test was run in duplicate. During the first tests with the 10 M, 5 M, and 3M NaOH solutions, a green Mn^{6+} species penetrated the glass frit of the Ag/AgCl reference electrodes. In order to prevent any shift in the reference electrode potential, a salt bridge was used with a SCE.[b] The initial OCP measurements were collected for 30 minutes for the solutions that did not contain sludge simulant. The

[b] The Ag/AgCl reference electrode is about 42 mV less than the SCE.

time was increased when the sludge was introduced up to 2 hours to allow time for the potential to stabilize. Figure 20 through Figure 23 display the data collected for the initial OCP measurements.

The OCP values are significantly more noble than those values that would be observed in either a simple sodium hydroxide solution or nitric acid solution. This observation is reflective of the permanganate, which is a strong oxidizer. The potentials are at values well above the value for hydrogen evolution. The potentials do become more noble as the pH decreases.

The addition of the simulant to the cleaning solutions did not impact the OCP more than 100 mV for the most extreme case. The 5 M NaOH solutions with HM and the PUREX showed the greatest separation at 106 mV at the most extreme values. The other 3 groups fall within a 60 mV window where the greatest variation between the maximum and minimum values is 55 mV.

Table 10. Open Circuit Measurements for Tests Described in Table 2.

Test	NaOH (M)	Simulant	OCP, mV vs. SCE
1[1]	10	None	246[2]
Dup[1]	10	None	243[2]
2	10	PUREX	238
Dup	10	PUREX	224
3	10	HM	241
Dup	10	HM	279
4[2]	5	None	342[2]
Dup[1]	5	None	375[2]
5	5	PUREX	344
Dup	5	PUREX	352
6	5	HM	269
Dup	5	HM	269
7	3	None	407
Dup	3	None	404
8	3	PUREX	381
Dup	3	PUREX	367
9	3	HM	400
Dup	3	HM	378
0.18M HNO_3			
10	0.18	None	1197
Dup	0.18	None	1145
11	0.18	PUREX	1173
Dup	0.18	PUREX	1166
12	0.18	HM	1167
Dup	0.18	HM	1165

[1]Testing used a Ag:AgCl reference electrode.
[2]Adjusted to SCE reference value, i.e. +42 mV

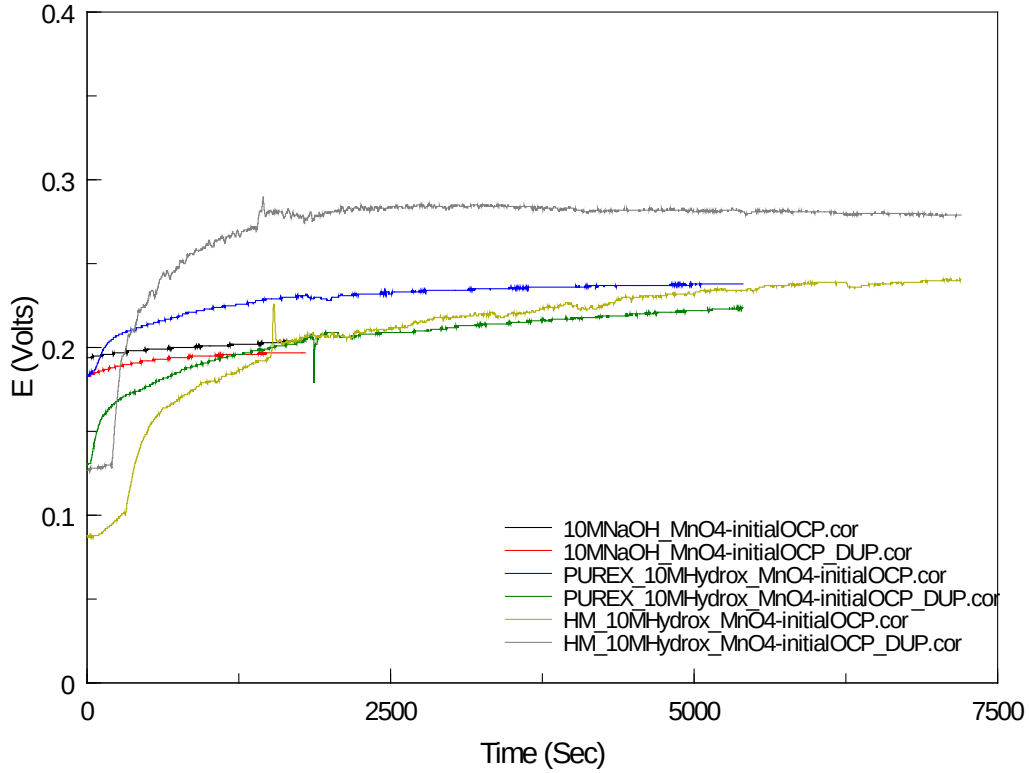

Figure 20. Open Circuit Potential Measurements vs. SCE for 10M NaOH: 0.05M $NaMnO_4$ Tests.

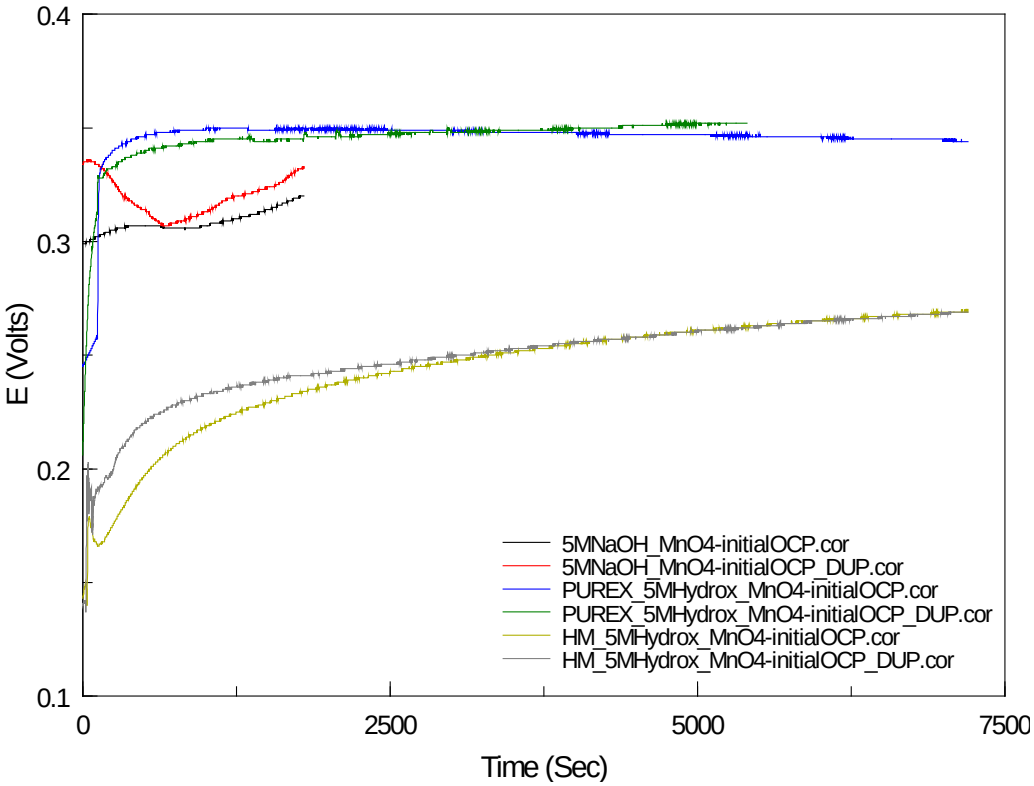

Figure 21. Open Circuit Potential Measurements vs. SCE for 5M NaOH: 0.05M NaMnO4 Tests.

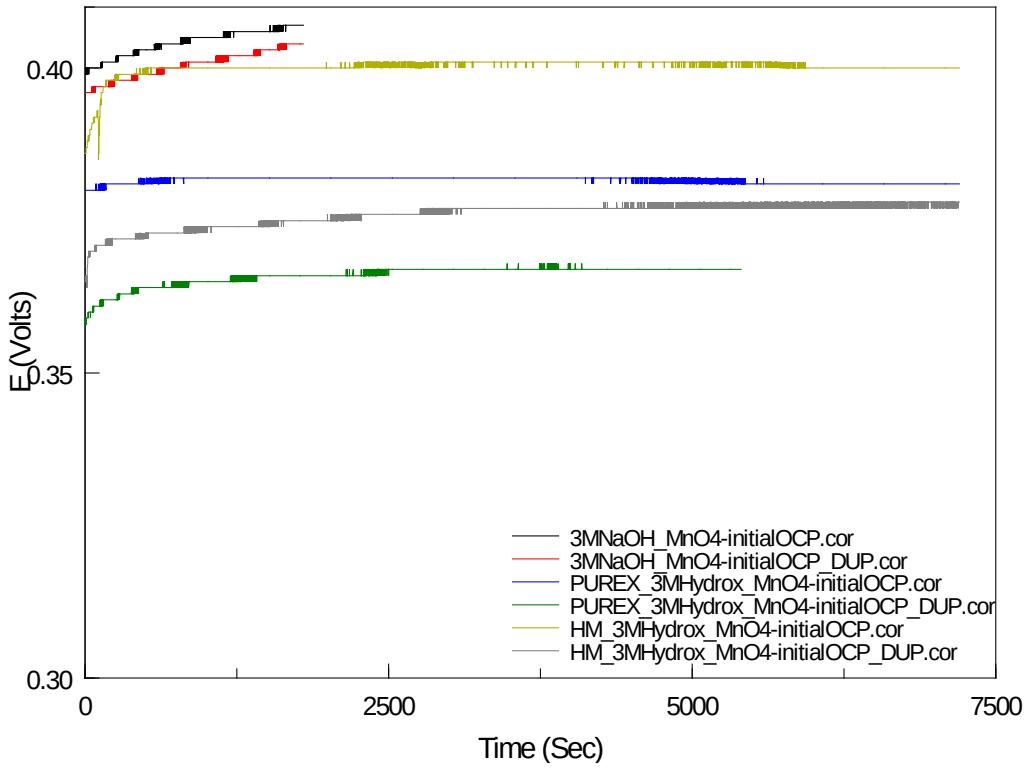

Figure 22. Open Circuit Potential Measurements vs. SCE for 3M NaOH: 0.05M NaMnO4 Tests.

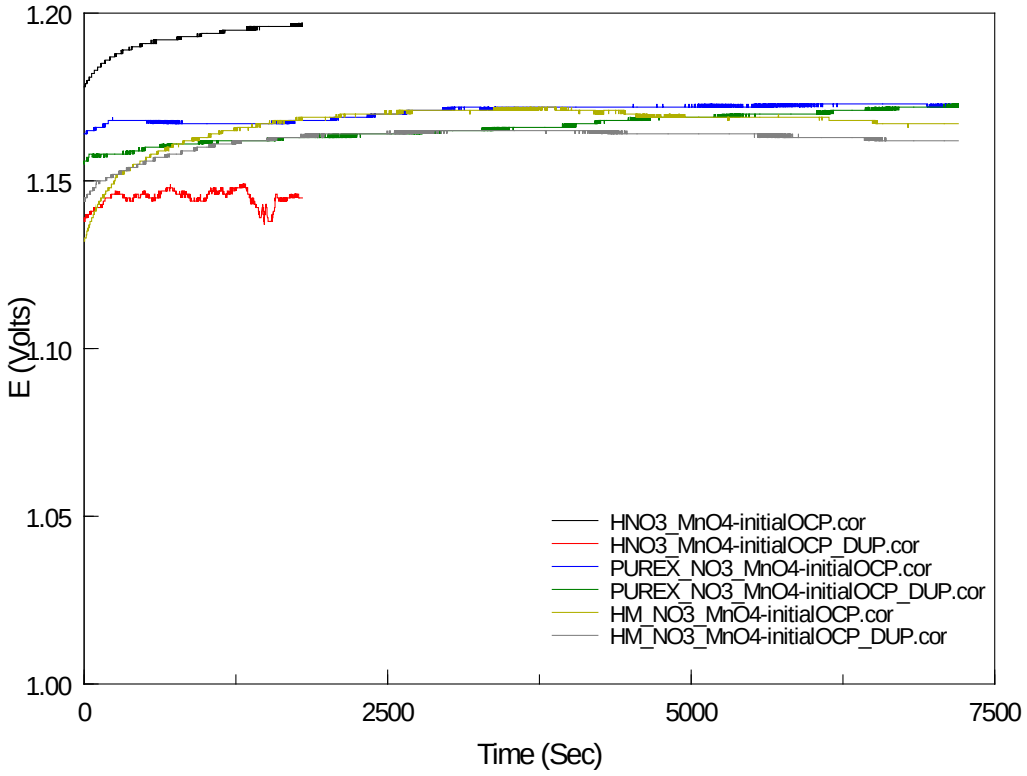

Figure 23. Open Circuit Potential Measurements vs. SCE for 0.18M HNO_3: 0.05M NaMnO4 Tests.

4.2.3 LPR and CPP results.

Table 11 gives the general corrosion rates for the LPR tests on the test solutions from Table 2. The corrosion rate was calculated from a polarization resistance fit discussed in Section 3.3.2. The highest corrosion rates found were for the 3M NaOH: 0.05M $NaMnO_4$ solution. These corrosion rates are very low, much lower than observed with the oxalic acid and oxalic acid/nitric acid blend, and would not present an issue. Coupon tests would be necessary to confirm, however, that a chemical dissolution mechanism is not occurring due to the presence of the strong oxidizer (i.e., permanganate).

The results of the CPP curves showed primarily active dissolution of the metal that reaches a high limiting current value with only a small degree of polarization. There was a slight indication of positive hysteresis in the CPP curve. It is possible the hysteresis could be an artifact of another process, such as deposition of a metal from solution.

Table 11. General Corrosion Rates for Sodium Hydroxide and Nitric Acid Solutions with 0.05M $NaMnO_4$ Mixed in a 20:1 Ratio with the Test Simulants for ASTM A285 Carbon Steel Performed at Room Temperature (22ºC ± 2°C).

Test	NaOH (M)	Simulant	Corrosion Rate (MPY)	CPP	
			LPR	Hysteresis	Notes:
1*	10	None	2.14	sl. Positive	
*Dup**	10	None	2.24	sl. Positive	
2	10	PUREX	2.99	sl. Positive	E_{rp} near E_{corr}
Dup	10	PUREX	3.79	sl. Positive	E_{rp} near E_{corr}
3	10	HM	1.22	sl. Positive	
Dup	10	HM	0.835	sl. Positive	
4*	5	None	0.878	Positive+	
*Dup**	5	None	0.869	Positive+	
5	5	PUREX	7.83	Positive+	E_{rp} near E_{corr}
Dup	5	PUREX	9.07	Positive+	E_{rp} near E_{corr}
6	5	HM	0.457	Positive+	
Dup	5	HM	1.12	Positive+	
7	3	None	22.5	Positive+	E_{rp} near E_{corr}
Dup	3	None	25.4	Positive+	E_{rp} near E_{corr}
8	3	PUREX	28.8	Positive+	$E_{rp} < E_{corr}$
Dup	3	PUREX	14.3	Positive+	$E_{rp} < E_{corr}$
9	3	HM	24.6	Positive+	$E_{rp} < E_{corr}$
Dup	3	HM	35.4	Positive+	$E_{rp} < E_{corr}$
0.18M HNO_3					
10	0.18	None	1.77	Positive+	
Dup	0.18	None	18.0	Positive+	
11	0.18	PUREX	2.73	Positive+	
Dup	0.18	PUREX	2.13	Positive+	
12	0.18	HM	1.17	Positive+	
Dup	0.18	HM	2.32	Positive+	$E_{rp} > E_{corr}$

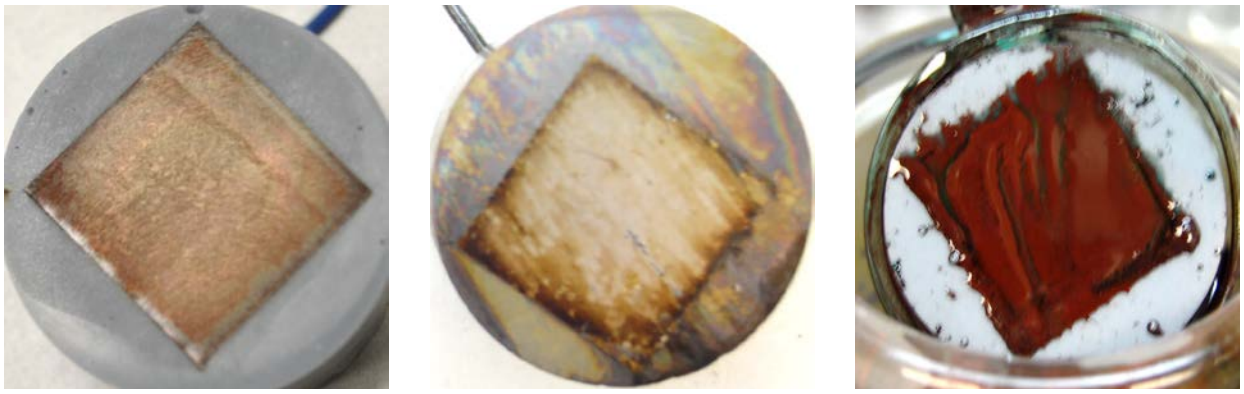

A **B** **C**

Figure 24. Photos of Electrodes Post Electrochemical Testing Using Sodium Permanganate.

The working electrode from each test had a deposit on the coupon surface, as can be observed in Figure 24. In Figure 24 A, the photograph was taken post testing with the 10M NaOH: $NaMnO_4$ solution and no simulant. The film was chemically adhered to the surface and could not be removed with water or by rubbing. In Figure 24 B, this image captures the results after testing with the 0.18M HNO_3: $NaMnO_4$ solution. In this instance, the film could be removed partially by rubbing the residue with a paper towel. In Figure 24 C, the image shows the result of 3M NaOH: $NaMnO_4$ with PUREX simulant. In this test, the simulant could be washed away with a stream of water leaving a film similar to that observed in Figure 24 A. It is possible these films cause a higher resistance and result in the higher current density than is observed in the CPP curves shown in Figure 25 through Figure 28. It is not known whether this is either deposition of solids from the simulant slurry or chemical dissolution of the electrode material.

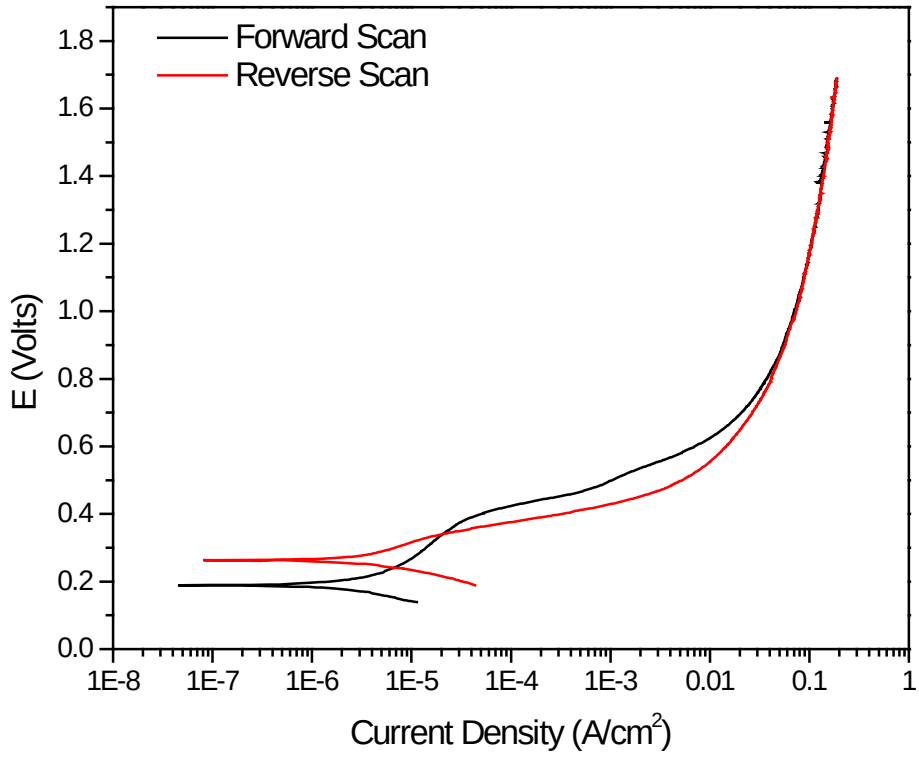

Figure 25. Cyclic Potentiodynamic Polarization Plot of 10 M NaOH: 0.05 M $NaMnO_4$.

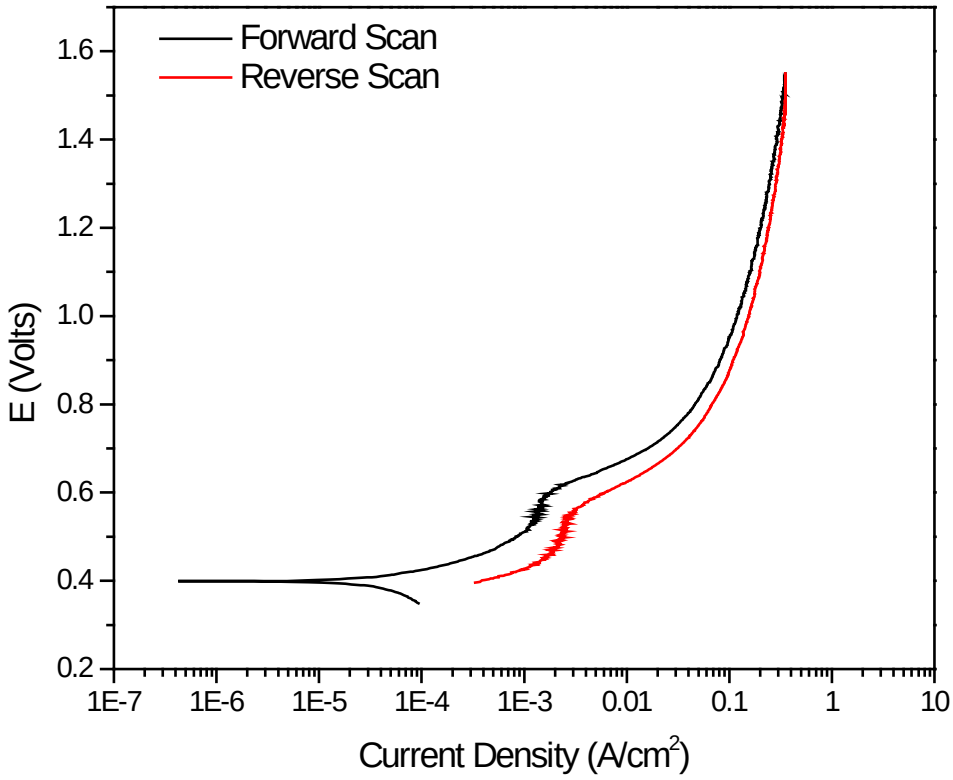

Figure 26. Cyclic Potentiodynamic Polarization Plot of 3 M NaOH: 0.05 M $NaMnO_4$ with HM Simulant.

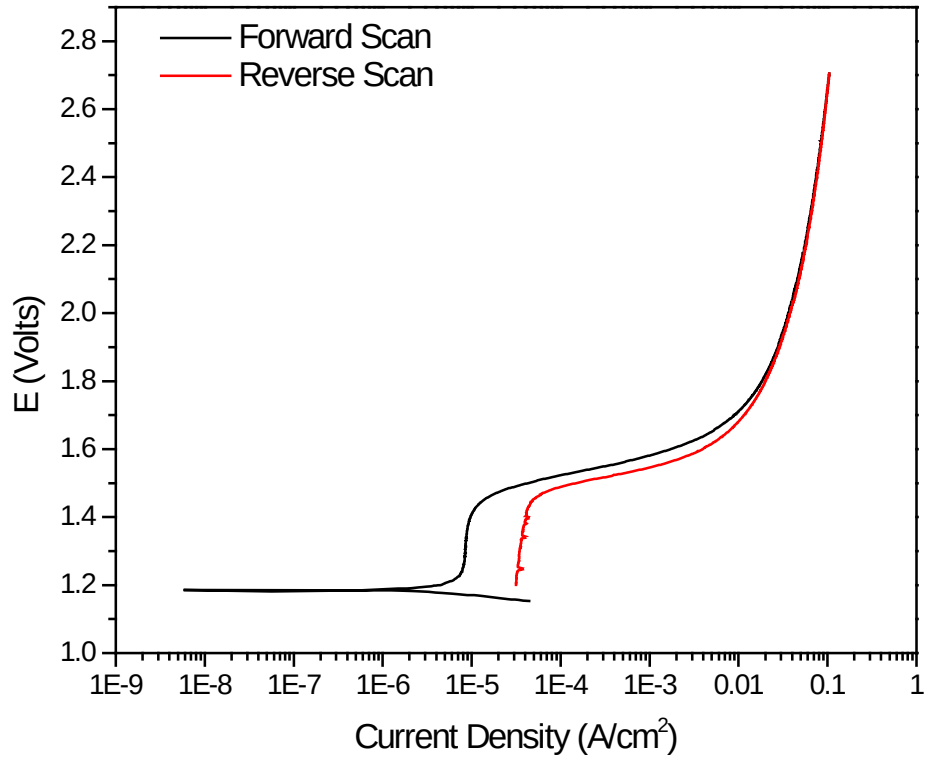

Figure 27. Cyclic Potentiodynamic Polarization Plot of 0.18M HNO_3: 0.05 M $NaMnO_4$.

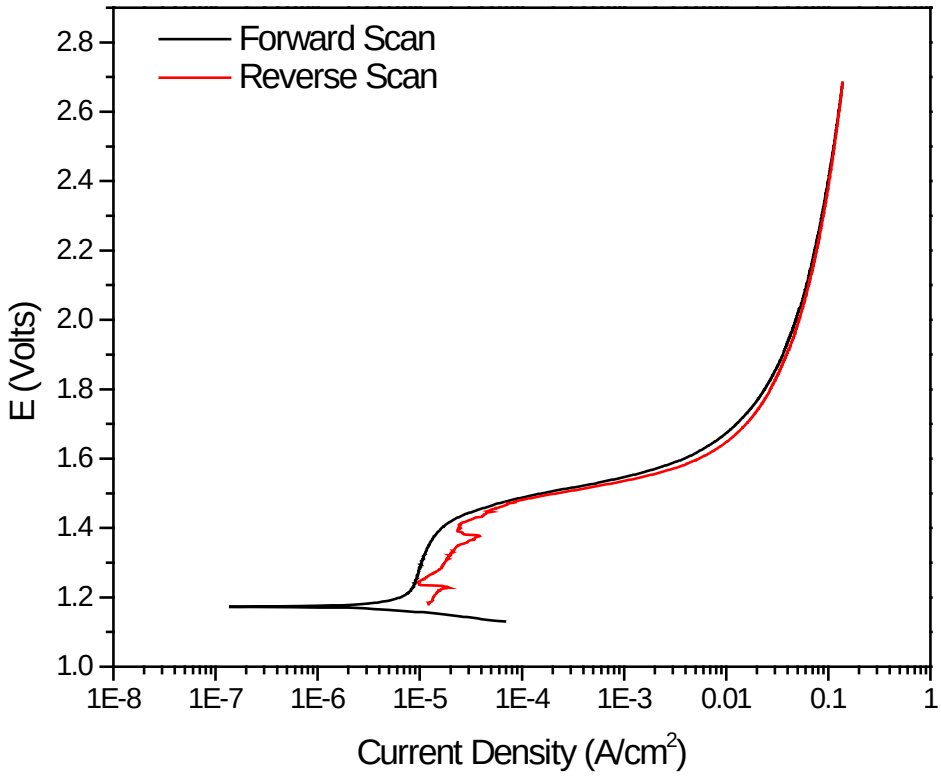

Figure 28. Cyclic Potentiodynamic Polarization Plot of 0.18 M HNO_3: 0.05 M NaMnO4 with PUREX Simulant.

4.2.4 Cathodic polarization testing.

Table 12 gives the results of the cathodic polarization testing results. The purpose of this testing is to determine the kinetics of the cathodic reaction and if hydrogen will be evolved as an active process when the acid interacts with the waste. In order for hydrogen evolution to occur, the value a must be within a specific range as discussed in Section 3.3.2.3 and below the potential for the hydrogen reduction reaction. In the basic conditions, where the potential is the lowest, the potential is positive for all solutions with respect to SCE. Therefore, the free potential is too noble for hydrogen evolution. Permanganate reduction or oxygen evolution are the more likely candidates for the cathodic reaction.

Table 12. Cathodic Polarization Parameters for Hydroxide and Nitric Acid Solution Testing.

	β (mV/decade)	I_o (Amp/cm^2)	E_o (Volts)[a]	α
10M NaOH				
No Simulant	-98.7	3.87E-06	0.209[b]	0.59
	-86.7	4.09E-06	0.200[b]	0.67
PUREX	-61.6	4.14E-06	0.238	0.94
	-78.6	7.57E-06	0.225	0.74
HM	-79.0	3.58E-06	0.240	0.74
	-77.0	2.41E-06	0.276	0.76
5M NaOH				
No Simulant	-143.9	1.83E-06	0.329[b]	0.40
	-149.7	1.99E-06	0.342[b]	0.39
PUREX	-155.4	1.31E-05	0.343	0.37
	-155.7	1.51E-05	0.351	0.37
HM	-60.3	5.57E-07	0.271	0.97
	-65.5	2.13E-06	0.271	0.89
3M NaOH				
No Simulant	-141.2	2.61E-05	0.407[b]	0.41
	-168.7	4.31E-05	0.397[b]	0.34
PUREX	-105.9	3.16E-05	0.381	0.55
	-103.8	1.98E-05	0.366	0.56
HM	-117.6	3.66E-05	0.400	0.49
	-122.3	5.54E-05	0.377	0.48
0.18M Nitric Acid				
No Simulant	-44.1	2.29E-06	1.198	1.32
	-63.9	4.12E-05	1.137	0.91
PUREX	-39.4	3.42E-06	1.172	1.48
	-40.3	2.53E-06	1.173	1.44
HM	-46.3	1.82E-06	1.166	1.26
	-48.3	3.88E-06	1.160	1.21

[a.] Potential versus SCE
[b.] Potential versus Ag/AgCl

5 Conclusions

The testing presented in this report examined the corrosion of A285 carbon steel exposed to a chemical cleaning solution composed of 0.18M nitric acid and 0.5 wt. % oxalic acid at 50℃. This solution has been proposed as a chemical cleaning solution for the hard heel portion of the sludge in the waste tanks. When this solution was combined with the HM or PUREX simulated sludge, the corrosion rates determined from passive coupon tests were nearly 500 mils per year in the worst case (for PUREX simulant at a 50:1 acid to sludge ratio), but decreased with time in 28-day tests. The highest corrosion rate determine by electrochemical probes was 76 mils per year (for HM 20:1.) The tests showed corrosion behavior to be active general corrosion.

Based on weight loss determination, the high acid to sludge ratio (50:1) results in a solution that is more corrosive than the low acid to sludge ratio (20:1). For example, the corrosion rates for the PUREX simulant at a 50:1 ratio ranged from approximately 250 to 490 MPY, whereas for the 20:1 ratio the rates ranged from approximately 120 to 240 MPY. A similar trend was observed for the HM simulant. Additionally, the dissolution of the PUREX sludge results in a simulant that is more corrosive than the solution that results from dissolution of the HM sludge.

Both dissolved sludge simulants resulted in similar trends in solution corrosivity and metal corrodibility. The ratio of acid to sludge determined the evolution of the solution corrosivity and metal corrodibility. For the 20:1 acid to sludge ratio, the solution corrosivity increases with time, whereas for the 50:1 ratio the solution corrosivity decreases with time. For both 20:1 and 50:1 sludge ratios, metal corrodibility increases with time. This suggests that the ferric oxalate film that forms on the steel surface degrades with time and offers less protection.

Corrosion rates from the passive coupon tests for the nitric acid/oxalic acid blend are significantly greater than those from the LPR measurements. There are several factors that could contribute to this. This result may be due to simultaneous electrochemical and chemical dissolution of the steel. As a result, the results from the LPR tests would not be useful without significant correction. Further testing would be necessary to determine if chemical dissolution were a factor.

In comparison to previous testing[8], the integrated corrosion rate is about the same for the HM and PUREX simulants and a 0.1M nitric acid and 1 wt. % oxalic acid cleaning solution at 45 ℃. The corrosion rates determined by LPR were 87 MPY for the HM solution and 54 MPY for the PUREX solution, each a dilution of about 12:1, cleaning solution to simulant. Where the average integrated corrosion rate for the HM simulant solutions were 73 MPY for the 20:1 dilution and 62 MPY for the 50:1 dilution and 66 MPY and 46 MPY for the PUREX 20:1 and 50:1 dilutions, respectively. There were also differences in the testing method where previous testing used an initial rest time of 1 to 4 hrs, where this testing was performed over 28 days and the first LPR was performed after 5 days.

The corrosion rate data from the coupon tests in the nitric acid/oxalic acid blend would need to be evaluated to determine the degree of potential structural damage. The corrosion rates, although relatively high, would not be expected to cause damage that would reduce the capacity of the tank primary if the process is completed within a month.[1] The OCP measurements do indicate that hydrogen evolution is thermodynamically possible. However, further studies would be needed to determine the rate at which hydrogen evolution occurs.

The corrosivity of sodium permanganate in four proposed cleaning solutions, 1 nitric acid solution and 3 sodium hydroxide solutions, was studied by electrochemical methods at room temperature. The corrosion rates were less aggressive than in the oxalic acid tests. The most aggressive solution was the 3M sodium hydroxide with permanganate which had corrosion rates greater than 20 mils per year based on linear polarization tests. The cyclic potentiodynamic polarization tests indicated that primarily general corrosion occurs. Passive coupon tests need to be performed in these solutions to ensure that chemical dissolution of the metal is not occurring simultaneously.

The sodium permanganate solutions in the 5M and 10M sodium hydroxide solutions was observed to change oxidation state when the solution was allowed to equilibrate overnight. The deep purple permanganate ion was reduced to the green Mn^{6+} and blue Mn^{5+} species. The purple Mn^{+7} was recovered when the solutions were acidified or diluted with distilled water. The impcat of the metal oxidation state could be something to consider in future testing involving similar testing conditions.

6 References

1. Martin., K.B., “Evaluation of the Impact of Removing Corrosion Controls During Waste Tank Closure Activities”, C-ESR-F-00041, Rev. 5, March 2013.
2. Office of Tank Waste & Nuclear Materials (EM-20), Work Authorization/Task Change Request HQTD1001, Waste Retrieval and Closure Technologies, February 2014.
3. Suduth, C., J. Vitalli, M. Keefer, “Evaluation of Sludge Heel Dissolution Efficiency with Oxalic Acid Cleaning at Savannah River Site”, Waste Management 2014 Conference, Paper # 14205, March 2014.
4. Isom, S. T., A. G. Garrison. “Evaluation of the Impact of Oxalate Formation from Bulk Oxalic Acid Cleaning (BOAC) on the Concentration, Storage, and Transfer Facilities (CSTF) and Downstream Facilities”, X-ESR-G-00037, Rev. 0, March 2014.
5. King. W. D., M. S. Hay, “Alternative Enhanced Chemical Cleaning: Basic Studies Results FY09”, SRNL-STI-2009-00791, Rev. 0, February 2010.
6. King. W. D., M. S. Hay, “Alternative Enhanced Chemical Cleaning: Basic Studies Results FY10”, SRNL-STI-2010-00541, Rev. 0, January 2011.
7. King. W. D., M. S. Hay, “Real Waste Testing Recommendations for Sludge Heel Dissolution in Oxalic Acid”, L3100-2010-00203, Rev. 0, September 2010.
8. Wiersma, B. J., “Alternative and Enhanced Chemical Cleaning: Corrosion Studies Results FY10”, SRNL-STI-2010-00555, Rev. 0, September 2010.; Wiersma, B. J., “Treatment Tank Corrosion Studies for the Enhanced Chemical Cleaning Process”, SRNL-STI-2010-00535, Rev.1, August 2011.
9. Rudisill, T. S., M. C. Thompson, “Enhanced Chemical Cleaning of SRS Wastes to Improve Actinide Solubility”, SRNL-STI-2011-00521, Rev. 0, September 2011.
10. Eibling, R. E. “Development of Hazardous Sludge Simulants for Enhanced Chemical Cleaning Tests”, SRNL-STI-2010-00170, Rev. 0, April 2010.
11. ASTM G 59-97, “Standard Test Method for Conducting Potentiodynamic Polarization Resistance Measurements,” ASTM International, West Conshohocken, PA, 2014.
12. F. Mansfeld, “The Polarization Resistance Technique”, in Advances in Corrosion Science and Technology, Vol.6, eds. M. G. Fontana and R. W. Staehle, Plenum Press, New York, NY, 1976, p. 163.
13. ASTM G 1-03, “Standard Practice for Preparing, Cleaning, and Evaluating Corrosion Test Specimens,” ASTM International, West Conshohocken, PA, 2011.

14. Kolotyrkin, Y., et. al, "Role of Oxidizers in the Active Dissolution and Passivation of Metals",Electroanalytical Chem., Vol. 69, 1976, pp. 407-414.
15. (12) Rayner-Canham, Geoff, Descriptive Inorganic Chemistry, W.H. Freeman and Company, New York, pp. 423-427, 1996.

Appendix A
Photographs of Weight Loss Coupons Post-Test Cleaning

Test Solution	Coupon 1	Coupon 2	Coupon 3	Coupon 4
HM 20:1				
(front)		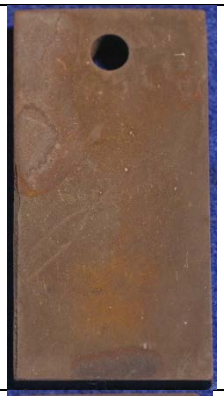		
(back)			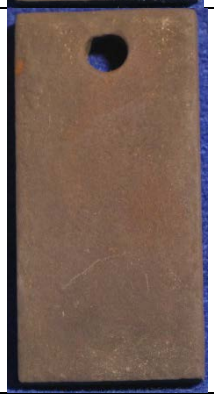	
HM 50:1				
(front)				
(back)				

Test Solution	Coupon 1	Coupon 2	Coupon 3	Coupon 4
PUREX 20:1				
(front)				
(back)				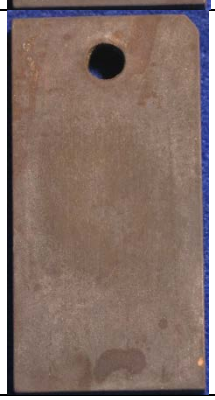
PUREX 50:1				
(front)				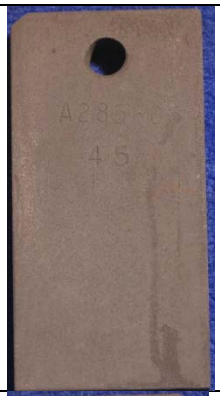
(back)				

Stainless Coupon Tests	HM 20:1	HM 50:1	PUREX 20:1	PUREX 50:1
2 Weeks				
4 Weeks				

Appendix B
Additional and Miscellaneous Data

Table B-1. Initial and Final Masses and Exposure Time of the Passive Weight Loss Coupons, given in grams.

Coupon	Time (Hrs)	HM 20:1		HM 50:1	
		Initial Mass	Final Mass	Initial Mass	Final Mass
1	168	59.7711	57.7402	55.4574	51.9198
2	384	57.4392	55.1296	58.7843	48.7869
3	672	55.8394	47.1922	60.9774	52.4829
4	168	58.7467	55.6343	59.1393	57.2905
		PUREX 20:1		PUREX 50:1	
		Initial Mass	Final Mass	Initial Mass	Final Mass
1	168	61.3258	58.1217	60.9063	54.4240
2	384	62.1126	58.5850	60.6651	53.0768
3	672	58.8521	50.5253	60.6306	44.0717
4	168	58.1286	55.0262	57.4650	55.3328

Table B-2. Analytical Chemistry Results for HM 20:1 Testing in mg/L.

Sample Time:	Week 1		Week 2		Week 4	
Sample ID:	20:1 HM-01	20:1 HM-01	20:1 HM-02	20:1 HM-02	20:1 HM-03	20:1 HM-03
Lab ID:	S-3069	S-3069	S-3070	S-3070	S-3071	S-3071
Analyte	mg/L	mg/L	mg/L	mg/L	mg/L	mg/L
Al	1510	1570	1000	987	623	645
B	<1.00	<1.00	<1.00	<1.00	<1.00	<1.00
Ba	18.4	18.4	18.0	18.0	17.5	17.6
Ca	18.7	18.8	23.1	22.9	22.9	22.9
Cd	<0.100	<0.100	<0.100	<0.100	<0.100	<0.100
Ce	10.3	10.2	8.71	8.72	7.81	7.81
Cr	27.2	27.1	3.05	3.04	1.24	1.24
Cu	9.28	9.28	0.656	0.653	0.484	0.482
Fe	53.2	53.2	919	910	1410	1440
K	6.99	7.04	88.0	88.7	96.1	97.1
La	2.50	2.50	2.28	2.26	2.05	2.05
Li	25.9	26.0	25.6	25.5	24.4	24.5
Mg	66.1	65.9	66.9	67.2	67.6	67.4
Mn	536	541	586	580	579	600
Na	208	209	220	216	210	218
Ni	59.2	59.3	61.0	60.9	61.2	61.2
P	<1.00	<1.00	<1.00	<1.00	<1.00	<1.00
Pb	26.3	26.3	6.32	6.36	4.37	4.30
Pd	<1.00	<1.00	<1.00	<1.00	<1.00	<1.00
S	4.93	4.74	1.74	1.68	1.62	1.48
Si	24.7	24.6	6.38	6.42	4.01	3.91
Sn	11.2	11.1	1.26	1.26	0.496	0.430
Ti	<1.00	<1.00	<1.00	<1.00	<1.00	<1.00
Zn	8.08	8.00	8.19	8.15	7.80	7.83
Zr	2.28	2.29	<0.100	<0.100	<0.100	<0.100
Hg	34.8	32.2	17.3	17.1	9.86	9.18

Table B-3. Analytical Chemistry Results for HM 50:1 Testing in mg/L.

Sample Time:	Week 1		Week 2		Week 4	
Sample ID:	50:1 HM-01	50:1 HM-01	50:1 HM-02	50:1 HM-02	50:1 HM-03	50:1 HM-03
Lab ID:	S-3072	S-3072	S-3073	S-3073	S-3074	S-3074
Analyte	mg/L	mg/L	mg/L	mg/L	mg/L	mg/L
Al	790	785	599	623	620	613
B	<1.00	<1.00	<1.00	<1.00	<1.00	<1.00
Ba	7.78	7.75	4.13	4.11	4.04	4.07
Ca	8.96	8.96	8.58	8.63	8.73	8.63
Cd	<0.100	<0.100	<0.100	<0.100	<0.100	<0.100
Ce	3.65	3.63	<1.00	<1.00	<1.00	<1.00
Cr	8.60	8.61	6.58	6.55	6.57	6.60
Cu	4.20	4.20	4.71	4.71	3.55	3.54
Fe	116	115	2890	2860	2800	2720
K	4.13	4.15	64.6	63.8	74.4	74.6
La	0.769	0.767	<0.100	<0.100	<0.100	<0.100
Li	9.01	9.01	6.06	6.07	6.05	6.02
Mg	23.0	22.9	13.8	13.8	13.9	14.0
Mn	197	195	162	169	175	173
Na	81.7	82.0	48.5	48.3	48.9	49.1
Ni	28.1	28.0	19.2	19.4	19.3	19.2
P	<1.00	<1.00	<1.00	<1.00	<1.00	<1.00
Pb	9.41	9.38	<1.00	<1.00	<1.00	<1.00
Pd	<1.00	<1.00	<1.00	<1.00	<1.00	<1.00
S	4.48	4.63	<1.00	<1.00	<1.00	<1.00
Si	8.77	8.63	6.22	6.21	6.85	6.91
Sn	3.42	3.39	2.28	2.25	2.25	2.35
Ti	<1.00	<1.00	<1.00	<1.00	<1.00	<1.00
Zn	2.87	2.87	1.90	1.92	1.87	1.85
Zr	15.8	15.8	<0.100	<0.100	<0.100	<0.100
Hg	9.40	8.52	14.7	14.1	12.0	11.6

Table B-4. Analytical Chemistry Results for PUREX 20:1 Testing in mg/L.

Sample Time:	Week 1		Week 2		Week 4	
Sample ID:	20:1 PU-01	20:1 PU-01	20:1 PU-02	20:1 PU-02	20:1 PU-03	20:1 PU-03
Lab ID:	S-3075	S-3075	S-3076	S-3076	S-3077	S-3077
Analyte	mg/L	mg/L	mg/L	mg/L	mg/L	mg/L
Al	1170	1240	973	964	739	771
B	<1.00	<1.00	<1.00	<1.00	<1.00	<1.00
Ba	5.83	5.78	16.6	16.7	16.0	16.0
Ca	42.3	42.0	44.1	44.3	43.4	43.2
Cd	<0.100	<0.100	<0.100	<0.100	<0.100	<0.100
Ce	45.5	45.3	28.2	28.1	24.8	24.7
Cr	0.121	0.103	0.671	0.655	0.651	0.664
Cu	12.0	12.1	0.267	0.267	1.28	1.28
Fe	202	213	2170	2110	2180	2160
K	3.16	3.11	64.2	63.7	70.9	71.5
La	11.964	11.838	8.22	8.29	7.29	7.25
Li	5.19	5.19	5.12	5.14	4.96	4.90
Mg	6.08	6.03	6.27	6.28	6.14	6.13
Mn	281	295	341	339	330	345
Na	51.9	51.4	55.9	55.5	53.1	53.8
Ni	420	439	403	400	299	314
P	<1.00	<1.00	<1.00	<1.00	<1.00	<1.00
Pb	17.7	17.7	5.18	5.14	3.77	3.80
Pd	<1.00	<1.00	<1.00	<1.00	<1.00	<1.00
S	7.50	7.42	3.04	2.93	2.46	2.34
Si	5.63	6.58	5.30	5.41	4.95	4.90
Sn	<0.100	<0.100	<0.100	<0.100	<0.100	<0.100
Ti	<1.00	<1.00	<1.00	<1.00	<1.00	<1.00
Zn	23.2	23.2	19.9	20.5	15.3	15.2
Zr	<0.100	<0.100	<0.100	<0.100	<0.100	<0.100
Hg	58.0	62.4	5.38	4.63	5.41	5.27

Table B-5. Analytical Chemistry Results for PUREX 20:1 Testing in mg/L.

Sample Time:	Week 1		Week 2		Week 4	
Sample ID:	50:1 PU-01	50:1 PU-01	50:1 PU-02	50:1 PU-02	50:1 PU-03	50:1 PU-03
Lab ID:	S-3078	S-3078	S-3079	S-3079	S-3080	S-3080
Analyte	mg/L	mg/L	mg/L	mg/L	mg/L	mg/L
Al	520	507	404	423	341	336
B	<1.00	<1.00	<1.00	<1.00	<1.00	<1.00
Ba	7.07	7.05	5.51	5.49	5.33	5.34
Ca	16.7	16.8	23.5	23.5	24.0	23.9
Cd	<0.100	<0.100	<0.100	<0.100	<0.100	<0.100
Ce	18.0	18.0	4.693	4.687	3.721	3.703
Cr	<0.100	<0.100	1.03	1.03	0.897	0.911
Cu	4.60	4.60	0.904	0.911	0.113	0.112
Fe	322	314	1440	1430	1550	1500
K	2.85	2.92	81.5	80.6	94.4	93.8
La	4.64	4.64	1.43	1.44	1.13	1.12
Li	2.82	2.82	2.88	2.88	2.89	2.89
Mg	1.68	1.67	1.96	1.94	2.05	2.04
Mn	124	121	183	191	200	198
Na	22.7	23.0	24.9	24.5	29.9	29.6
Ni	193	186	175	183	166	164
P	2.45	2.62	<1.00	<1.00	<1.00	<1.00
Pb	7.19	7.21	<1.00	<1.00	<1.00	<1.00
Pd	<1.00	<1.00	<1.00	<1.00	<1.00	<1.00
S	8.54	8.37	<1.00	<1.00	<1.00	<1.00
Si	1.07	1.01	1.72	1.76	1.93	1.84
Sn	<0.100	<0.100	0.130	0.118	0.140	0.121
Ti	<1.00	<1.00	<1.00	<1.00	<1.00	<1.00
Zn	9.08	9.00	7.90	8.02	6.95	6.95
Zr	<0.100	<0.100	<0.100	<0.100	<0.100	<0.100
Hg	33.6	34.7	1.07	1.10	<1.00	<1.00